

Mathematical modeling of an immune checkpoint inhibitor and its synergy with an immunostimulant

Based on:

- 1) E. Nikolopoulou, L.R. Johnson, D. Harris, J.D. Nagy, E.C. Stites, Y. Kuang, 2018. Tumour-immune dynamics with an immune checkpoint inhibitor. Letters in Biomathematics.
 - 2) E. Nikolopoulou, S. E. Eikenberry, J. L. Gevertz, Y. Kuang 2021. Mathematical modeling of an immune checkpoint inhibitor and its synergy with an immunostimulant. DCDS- B. 26 (4).
-

Yang Kuang

Jul 28 - Aug 1, 2025

ICERM

◆ AI Overview

Immune checkpoint therapy is a **type of cancer treatment that uses drugs to help the body's immune system fight cancer**. It works by blocking proteins called immune checkpoints, which cancer cells can use to evade the immune system. By blocking these checkpoints, the therapy allows T cells, a type of immune cell, to recognize and attack cancer cells more effectively. [🔗](#)

Here's a more detailed explanation:

How it works:

Immune Checkpoints:

Immune checkpoints are proteins on immune cells (like T cells) that act as "off switches" to regulate the immune response. They prevent the immune system from attacking healthy cells by dampening the immune response when it's no longer needed. [🔗](#)

Cancer's Trick:

Cancer cells can exploit these checkpoints by producing proteins (like PD-L1) that bind to checkpoint proteins on T cells, effectively telling the T cells to ignore the cancer cells. [🔗](#)

Checkpoint Inhibitors:

Immune checkpoint inhibitors are drugs that block these checkpoint proteins, preventing them from interacting with cancer cells. This allows the T cells to become activated and attack the cancer cells. [🔗](#)

Types of Checkpoint Inhibitors:

Common checkpoint inhibitors target proteins like CTLA-4, PD-1, and PD-L1. For example, ipilimumab and tremelimumab are CTLA-4 inhibitors, while nivolumab, pembrolizumab, atezolizumab, avelumab, and durvalumab are PD-1 or PD-L1 inhibitors. [🔗](#)

Combination Therapies:

Checkpoint inhibitors can also be used in combination with other treatments, such as chemotherapy or targeted therapy, to enhance their effectiveness. [🔗](#)

Effectiveness and Considerations:

Benefits:

Immune checkpoint inhibitors have shown remarkable success in treating various cancers, including melanoma, lung cancer, and some types of bladder, kidney, and head and neck cancers.

Predictive Biomarkers:

Researchers are actively working on identifying biomarkers (like PD-L1 expression) that can help predict which patients are most likely to respond to checkpoint inhibitors.

Side Effects:

Checkpoint inhibitors can cause side effects, including inflammation in various parts of the body, as they boost the immune response. These side effects can range from mild to severe and may require management with medications or other therapies.

Limitations:

Not all patients respond to checkpoint inhibitors, and some may experience resistance to these treatments.

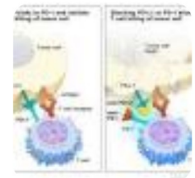
In summary, immune checkpoint therapy is a powerful tool in the fight against cancer, but it's not a one-size-fits-all solution and requires careful consideration of individual patient factors and potential side effects.

Immune Checkpoint Inhibitors - NCI

Apr 7, 2022 — What side effects are caused by immune checkpoint inhibitors?

Immune checkpoint inhibitors can cause side effects that ...

 National Cancer Institute



Immune Checkpoint Inhibitors and Their Side Effects

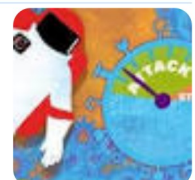
Dec 27, 2024 — Atezolizumab (Tecentriq and Tecentriq Hybreza) Avelumab (Bavencio)

Durvalumab (Imfinzi) Both PD-1 and PD-L1 inhibitors...

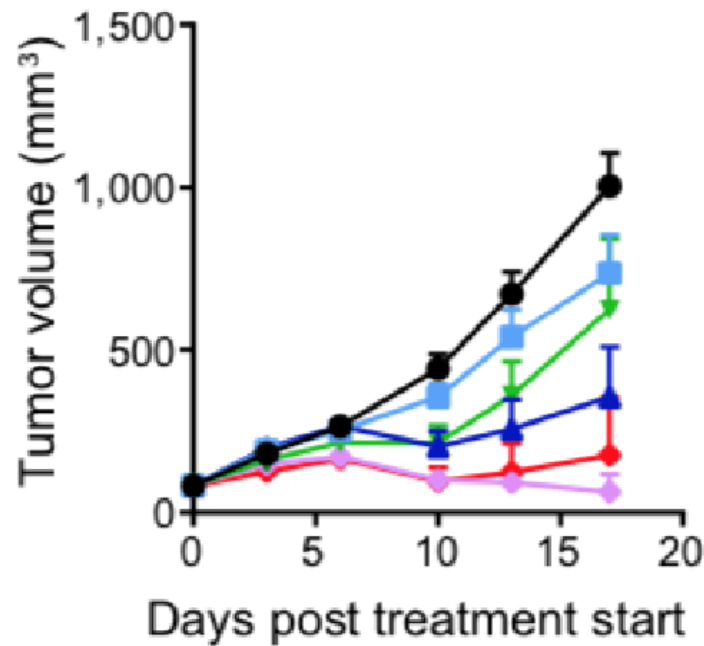
 American Cancer Society

What are Immune Checkpoint Inhibitors? Know Before Treatment | MD Anderson Cancer Center

 MD Anderson Cancer Center



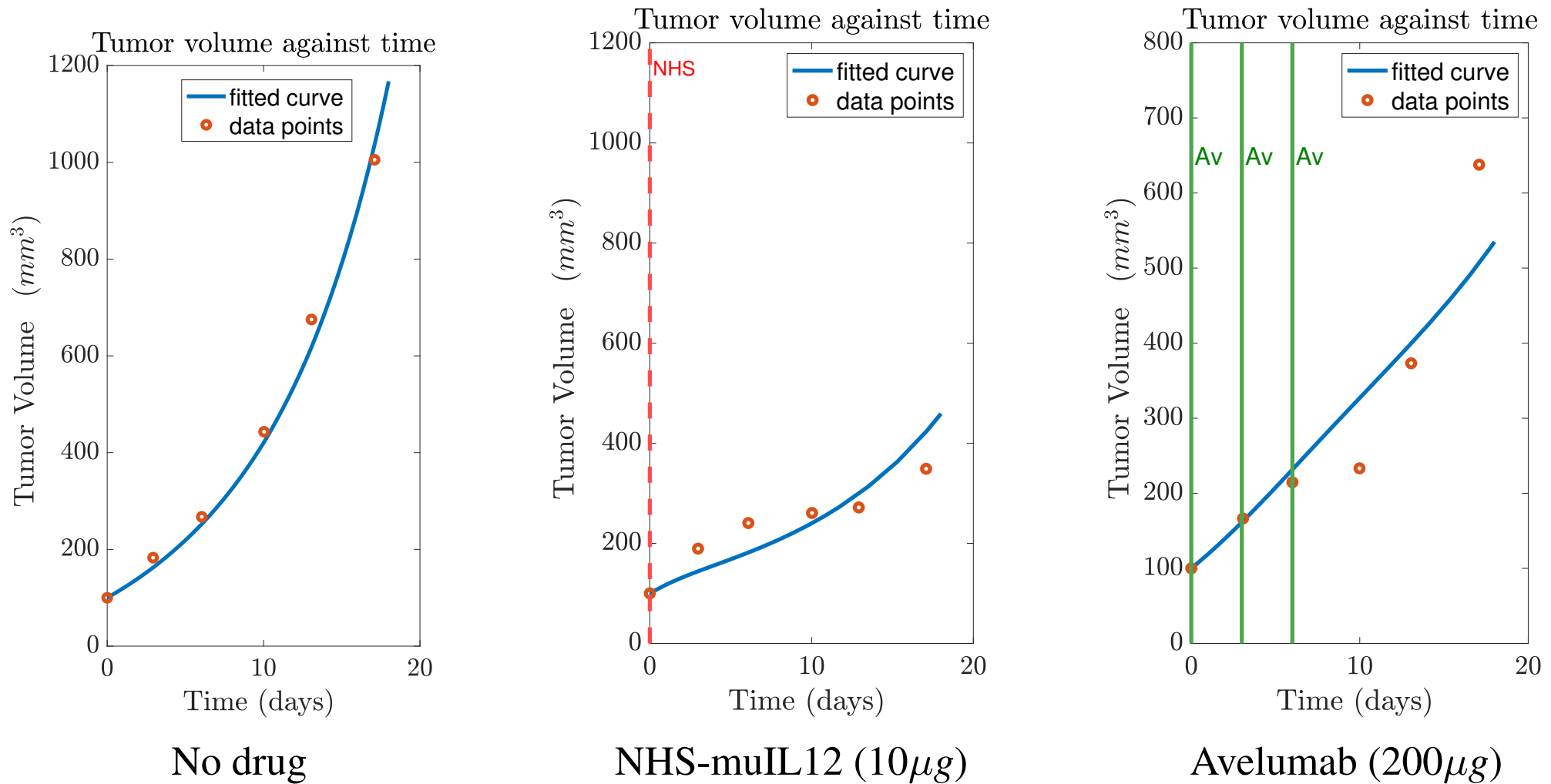
Experimental Mice Data in Xu et al. (2017)



- No drug
- NHS-muIL12 (2 µg)
- NHS-muIL12 (10 µg)
- Avelumab (200 µg)
- NHS-muIL12 (2 µg) + Avelumab (200 µg)
- NHS-muIL12 (10 µg) + Avelumab (200 µg)

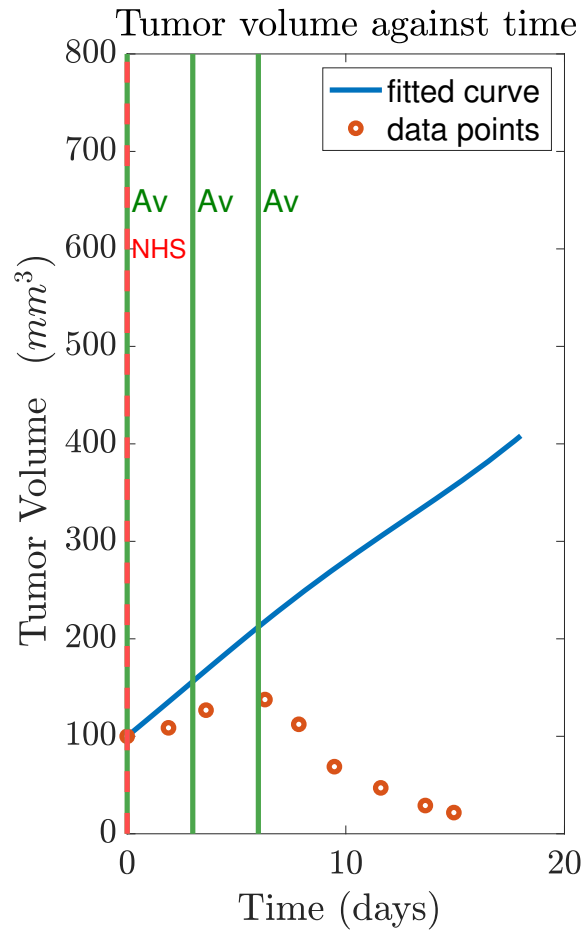
- Combination therapy enhanced antitumor efficacy compared to monotherapy.

Submodel Fits to Data: Monotherapy Treatment

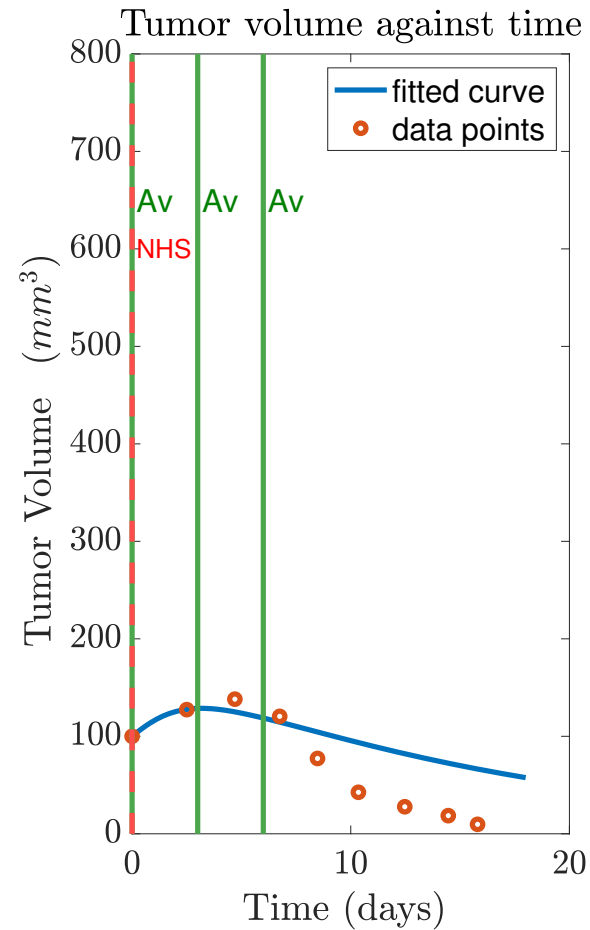


- Relatively good fits for the monotherapy case

Predictions: Combination Treatment



Av ($200\mu g$) + NHS ($2\mu g$)



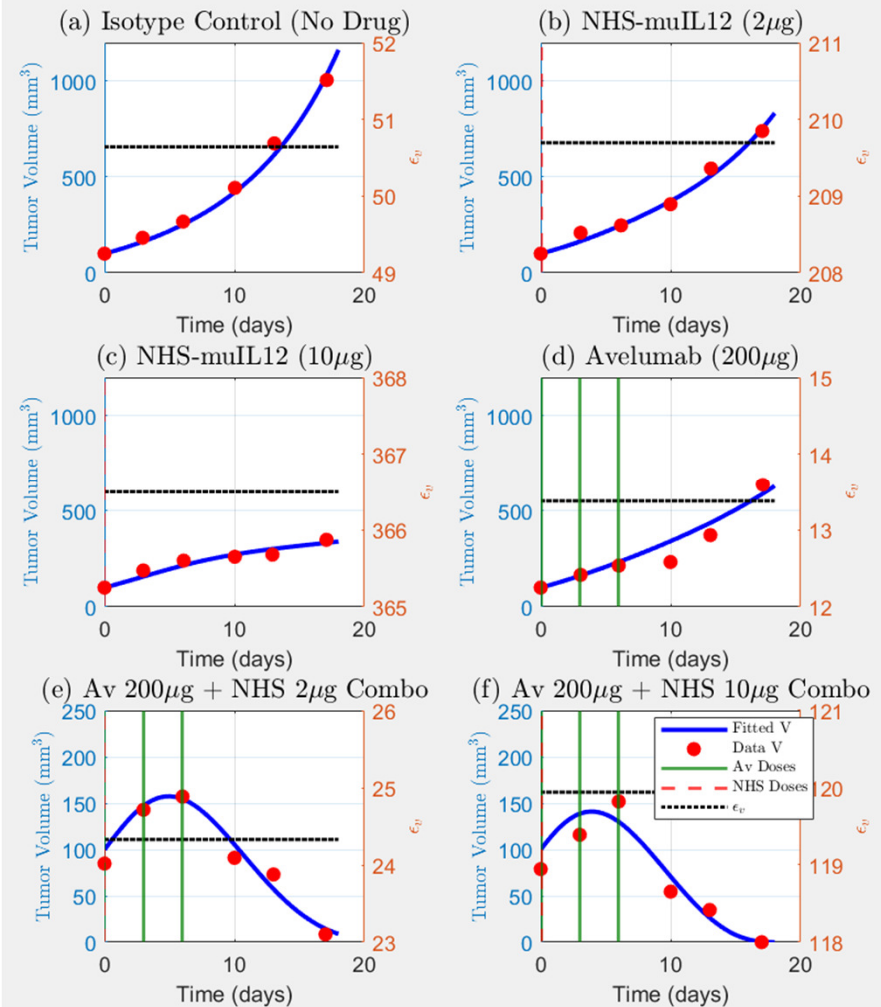
Av ($200\mu g$) + NHS ($10\mu g$)

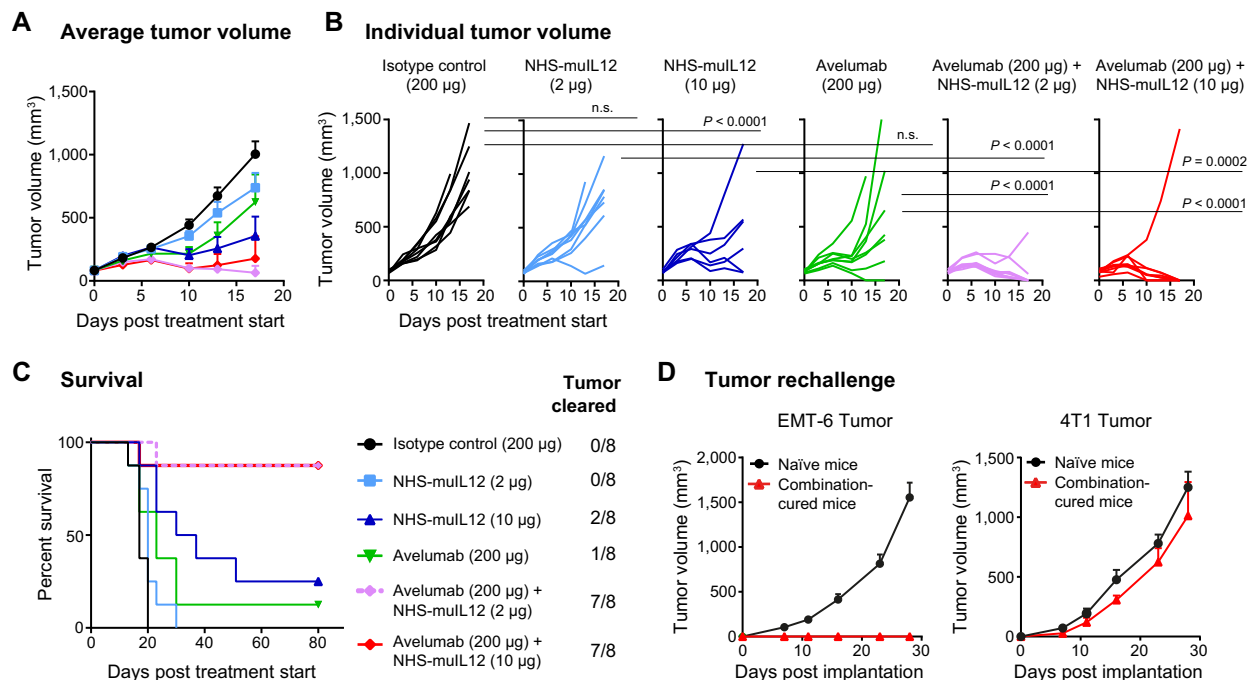
- Not qualitatively as good fits

Elpi's Original Model

- Constant epsilon, but fitted for each mode. Fits are very nice!
- Slight changes to her original parameters:
 - Incorporated the 3 new parameter values suggested earlier by Aigerim.
 - Set K_A1 and K_A2 to the estimated values that Elpi derived from literature, but decided not to use.
 - I let epsilon range from 1 to 400 in the fitting process.

4-ODE Model Individual Fits (ϵ_v)



**Figure 1.**

NHS-muL12 and avelumab combination treatment had a synergistic antitumor effect and induced long-term protective immunity in EMT-6 tumor-bearing mice. **A–C**, EMT-6 tumor-bearing BALB/c mice ($n = 8$ mice/group) were treated with: (i) isotype control (200 µg), (ii) NHS-muL12 (2 µg), (iii) NHS-muL12 (10 µg), (iv) avelumab (200 µg), (v) NHS-muL12 (2 µg) + avelumab (200 µg), or (vi) NHS-muL12 (10 µg) + avelumab (200 µg). NHS-muL12 was injected as a single subcutaneous dose on day 0, and avelumab or isotype control was administered intravenously on days 0, 3, and 6. **A**, Average tumor volumes, measured twice weekly. Error bars represent SEM. **B**, Individual tumor volumes, in which each line represents a single mouse. P values were calculated by two-way ANOVA followed by Bonferroni posttest. **C**, Kaplan-Meier survival curve and proportion of tumor clearance in each treatment group. **D**, Mice in complete remission for 3 months following last combination treatment (mice from two repeat studies) and naïve BALB/c mice were challenged with EMT-6 ($n = 20$ and 8, respectively) or 4T1 ($n = 5$ and 8, respectively) cells by orthotopic injection on the opposite mammary pad of the original tumor site. Average tumor volume after implantation. Error bars represent SEM. n.s., not significant.

Overview

The use of immune checkpoint inhibitors is becoming more commonplace in clinical trials across the nation. Two important factors in the tumor-immune response are the checkpoint protein programmed death-1 (PD-1) and its ligand PD-L1. We propose a mathematical tumor/immune model using a system of ordinary differential equations to study the dynamics of the system with and without the use of anti-PD-1, a checkpoint inhibitor which allows more T cells to recognize and fight tumor cells. A sensitivity analysis is conducted to determine the parameters driving the tumor burden. We consider the system without the anti-PD-1 drug to conduct a mathematical analysis of the model to determine the stability of the tumor-free and tumorous equilibria, comparing our findings with that of the simulations. Through simulations, we found that a normally functioning immune system may control tumor, in contrast to a weak immune system. When applying the treatment continuously, we observe treatment with anti-PD-1 alone may not be sufficient to eradicate the tumor cells.

Overview

The immune system works to differentiate between healthy cells and abnormal cells. Immune cells, known as T cells, fight the abnormal cells while leaving the healthy cells untouched. In accomplishing this, the use of “checkpoints”, molecules on immune cells that enhance or suppress an immune response, is employed.

Two important factors in the tumor-immune response are programmed death-1 (PD-1) and its ligand PD-L1. PD-1 is a protein expressed on activated T cells. PD-L1, found mainly on various types of tumor cells and T cells, is one of PD-1's ligands. When PD-1 binds to PD-L1, the PD-1-PD-L1 complex is formed, allowing the cell expressing PD-L1 to be unrecognized as a danger when detected. In response to an immune attack, tumor cells may overexpress PD-L1 and PD-L2 which can bind to PD-1 receptors on T cells, reducing or eliminating the effectiveness of T cells' attacks.

Some mathematical models of checkpoint inhibitor immunotherapies

1. H.G. Anderson, G.P. Takacs, D.C. Harris, Y. Kuang, J.K. Harrison and T.L. Stepien, 2024. Global stability and parameter analysis reinforce therapeutic targets of PD-L1-PD-1 and MDSCs for glioblastoma. *J. Math. Biol.*, 88:10.
2. S. Shi, J. Huang, Y. Kuang, S. Ruan, 2023. Stability and Hopf bifurcation of a tumor-immune system interaction model with an immune checkpoint inhibitor. *CNSNS*, Volume 118, 106996.
3. E. Nikolopoulou, S. E. Eikenberry, J. L. Gevertz, Y. Kuang 2021. Mathematical modeling of an immune checkpoint inhibitor and its synergy with an immunostimulant. *Discrete & Continuous Dynamical Systems - B*. 26 (4).
4. S. Shi, J. Huang, Y. Kuang 2021. Global dynamics in a tumor-immune model with an immune checkpoint inhibitor, *Discrete Continuous Dynamical Systems - B*. 26 (2), 1149-1170.
5. Elpiniki Nikolopoulou, Lauren R. Johnson, Duane Harris, John D. Nagy, Edward C. Stites and Yang Kuang, 2018. Tumour-immune dynamics with an immune checkpoint inhibitor, *Letters in Biomathematics*, DOI: 10.1080/23737867.2018.1440978

The Birth of Immunotherapy

New York Times - July 29, 1908

ERYSIPELAS GERMS AS CURE FOR CANCER

**Dr. Coley's Remedy of Mixed
Toxins Makes One Disease
Cast Out the Other.**

MANY CASES CURED HERE

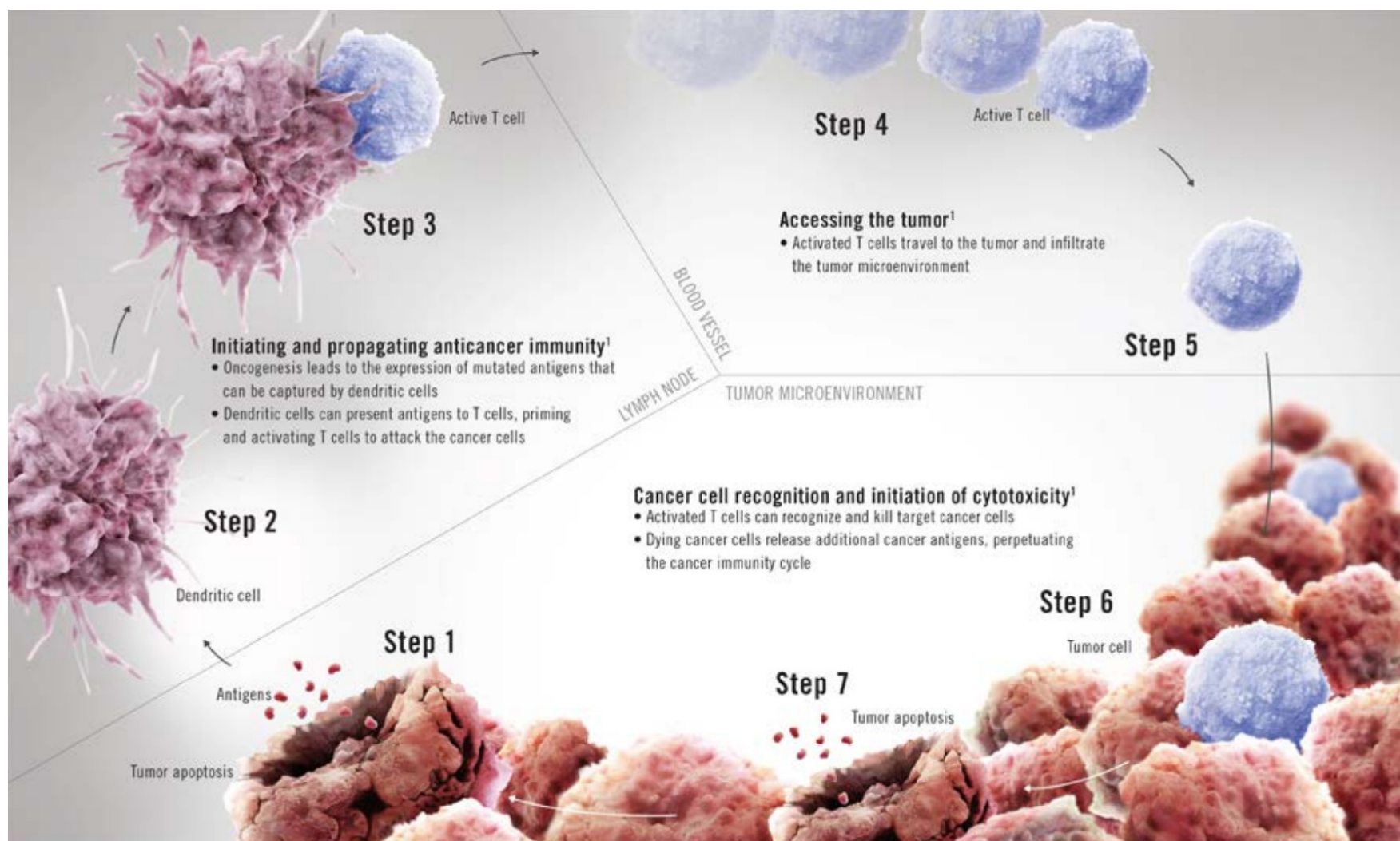
**Physician Has Used the Cure for 15
Years and Treated 430 Cases—
Probably 150 Sure Cures.**

Following news from St. Louis that
two men have been cured of cancer in
the City Hospital there by the use of
a fluid discovered by Dr. William B.
Coley of New York. It came out yester-

- Immunotherapy has been around for over 100 years, beginning most notably with “Coley’s Toxins”

Immunotherapy

Immunotherapy seeks to activate the immune system to fight cancer.



Immunotherapy Types

Main Types:

- Monoclonal antibodies
- Cancer vaccinations
- Immune checkpoint inhibitors
- Oncolytic virus therapy
- Other, Non-specific immunotherapies

Immune checkpoint Inhibitors:

- $\approx 600\%$ increase in clinical trials between 2015-2017
- $\approx 12.46\%$ patient response in 2017 compared to $\approx 0.14\%$ in 2011

Combination therapy of cancer with cancer vaccine and immune checkpoint inhibitors: A mathematical model

Xiulan Lai , Avner Friedman

Published: May 25, 2017 • <https://doi.org/10.1371/journal.pone.0178479>

Notation	Description	units
D	density of DCs	g/cm^3
T_1	density of activated CD4^+ T cells	g/cm^3
T_8	density of activated CD8^+ T cells	g/cm^3
C	density of cancer cells	g/cm^3
N_C	density of necrotic cancer cells	g/cm^3
H	HMGB-1 concentration	g/cm^3
G	GM-CSF concentration	g/cm^3
I_{12}	IL-12 concentration	g/cm^3
I_2	IL-2 concentration	g/cm^3
P	PD-1 concentration	g/cm^3
L	PD-L1 concentration	g/cm^3
Q	PD-1-PD-L1 concentration	g/cm^3
A	anti-PD-1 concentration	g/cm^3

<https://doi.org/10.1371/journal.pone.0178479.t001>

13 Partial Differential Equations

48 Parameters

$$\frac{\partial N_C}{\partial t} + \underbrace{\nabla \cdot (\mathbf{u} T_1)}_{\text{Velocity}} - \underbrace{\delta_{N_C} \nabla^2 N_C}_{\text{Diffusion}} = \underbrace{\lambda_{N_C} C C}_{\text{derived from life cancer cells}} - \underbrace{d_{N_C} N_C}_{\text{removal}} \quad (2.3.1)$$

$$\frac{\partial H}{\partial t} - \underbrace{\delta_H \nabla^2 H}_{\text{diffusion}} = \underbrace{\lambda_{N_H} N_C}_{\text{released from necrotic cancer cells}} - \underbrace{d_H H}_{\text{degradation}} \quad (2.3.2)$$

$$\frac{\partial D}{\partial t} + \underbrace{\nabla \cdot (\mathbf{u} D)}_{\text{Velocity}} - \underbrace{\delta_D \nabla^2 D}_{\text{Diffusion}} = \underbrace{\lambda_{D_C} D_0 \frac{C}{K_C + C}}_{\text{activation by HMGB-1}} - \underbrace{\lambda_{D_G} D_0 \frac{G}{K_G + G}}_{\text{promotion by GM-CSF}} - \underbrace{d_D D}_{\text{death}} \quad (2.3.3)$$

$$\begin{aligned} \frac{\partial T_1}{\partial t} + \nabla \cdot (\mathbf{u} T_1) - \delta_T \nabla^2 T_1 = & \left(\underbrace{\lambda_{T_1 I_{12}} T_{10} \frac{I_{12}}{K_{I_{12}} + I_{12}}}_{\text{activation by IL-12}} + \underbrace{\lambda_{T_1 I_2} T_1 \frac{I_2}{K_{I_2} + I_2}}_{\text{IL-2 induced proliferation}} \right) \\ & \times \underbrace{\frac{1}{1 + \frac{Q}{K_{TQ}}}}_{\text{inhibition by PD-1-PD-L1}} - \underbrace{d_{T_1} T_1}_{\text{death}} \end{aligned} \quad (2.3.4)$$

$$\begin{aligned} \frac{\partial T_8}{\partial t} + \nabla \cdot (\mathbf{u} T_8) - \delta_T \nabla^2 T_8 = & \left(\underbrace{\lambda_{T_8 I_{12}} T_{80} \frac{I_{12}}{K_{I_{12}} + I_{12}}}_{\text{activation by IL-12}} + \underbrace{\lambda_{T_8 I_2} T_8 \frac{I_2}{K_{I_2} + I_2}}_{\text{IL-2 induced proliferation}} \right) \\ & \times \underbrace{\frac{1}{1 + \frac{Q}{K_{TQ}}}}_{\text{inhibition by PD-1-PD-L1}} - \underbrace{d_{T_8} T_8}_{\text{death}} \end{aligned} \quad (2.3.5)$$

$$\frac{\partial C}{\partial t} + \nabla \cdot (\mathbf{u} C) - \delta_C \nabla^2 C = \underbrace{\lambda_C C \left(1 - \frac{C}{C_M}\right)}_{\text{proliferation}} - \underbrace{(\eta_1 T_1 C + \eta_8 T_8 C)}_{\text{killing by T cells}} - \underbrace{d_C C}_{\text{death}} \quad (2.3.6)$$

$$\frac{\partial G}{\partial t} - \delta_G \nabla^2 G = \underbrace{\lambda_G + \frac{G(t)}{K_G}}_{\text{injection}} - \underbrace{d_G G}_{\text{degradation}} \quad (2.3.7)$$

$$\frac{\partial I_{12}}{\partial t} - \delta_{I_{12}} \nabla^2 I_{12} = \underbrace{\lambda_{I_{12} D} D}_{\text{production by DCs}} - \underbrace{d_{I_{12}} I_{12}}_{\text{degradation}} \quad (2.3.8)$$

$$\frac{\partial I_2}{\partial t} - \delta_{I_2} \nabla^2 I_2 = \underbrace{\lambda_{I_2 T_1} T_1}_{\text{production by } T_1} - \underbrace{d_{I_2} I_2}_{\text{degradation}} \quad (2.3.9)$$

$$\begin{aligned} \frac{\partial P}{\partial t} - \nabla \cdot (\mathbf{u} P) - \delta_P \nabla^2 P = & \frac{P}{T_1 + T_8} (\lambda_{T_1 I_{12}} T_{10} + \lambda_{T_8 I_2} T_{80}) \frac{I_{12}}{K_{I_{12}} + I_{12}} \\ & + (\lambda_{T_1 I_2} T_1 + \lambda_{T_8 I_2} T_8) \frac{I_2}{K_{I_2} + I_2} \times \frac{1}{1 + \frac{Q}{K_{TQ}}} \\ & - \frac{P}{T_1 + T_8} (d_{T_1} T_1 + d_{T_8} T_8) - \underbrace{\mu_{PA} P A}_{\text{depletion by anti-PD-1}} \end{aligned} \quad (2.3.10)$$

$$L = \rho_L (T_1 + T_8 + \epsilon_C C) \quad (2.3.11)$$

$$\frac{\partial Q}{\partial t} - \nabla \cdot (\mathbf{u} Q) - \delta_Q \nabla^2 Q = \alpha_{PL} P L - d_Q Q \quad (2.3.12)$$

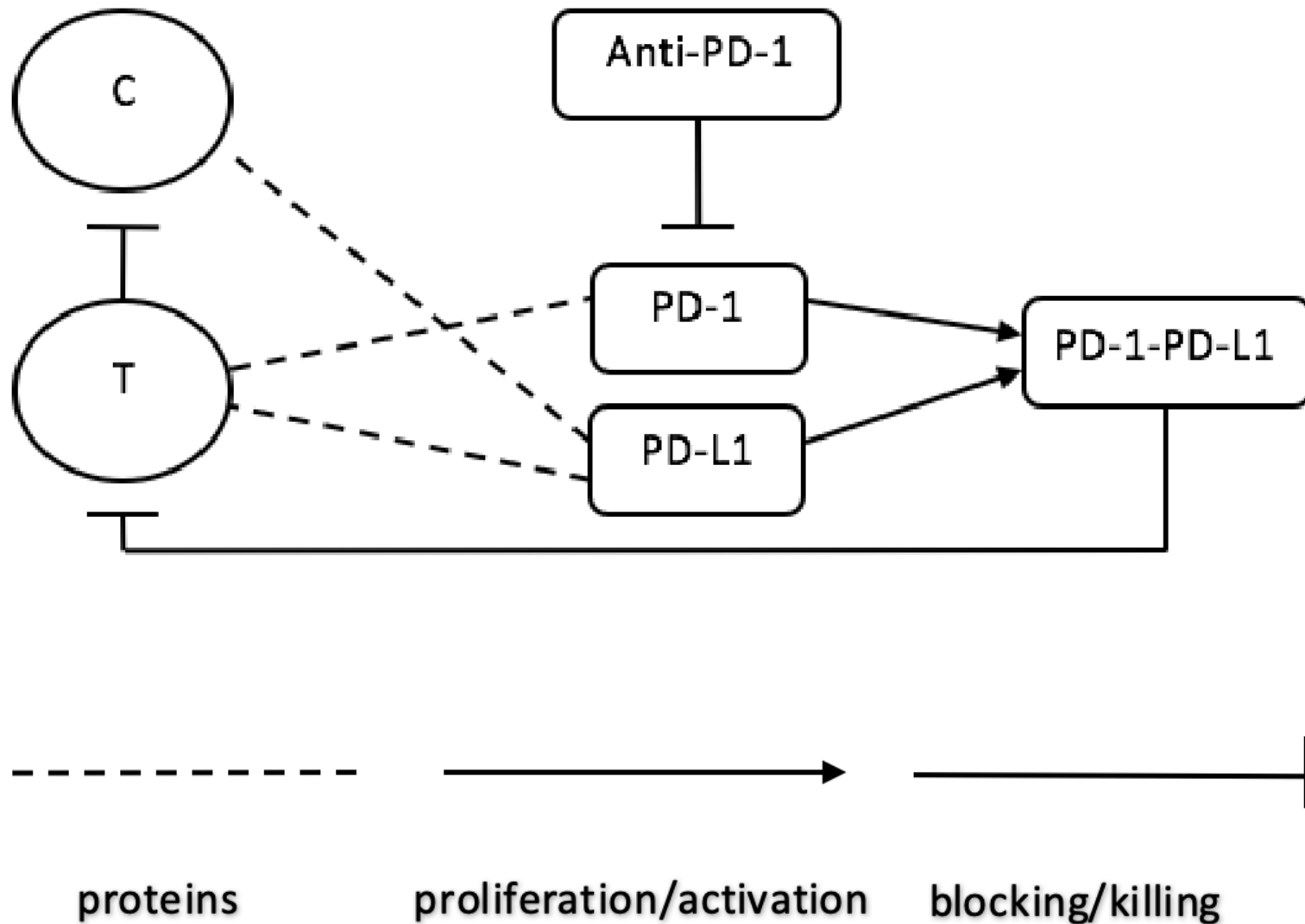
$$\frac{\partial A}{\partial t} - \delta_A \nabla^2 A = \underbrace{A(t)}_{\text{injection}} - \underbrace{\mu_{PA} P A}_{\text{depletion through blocking PD-1}} - \underbrace{d_A A}_{\text{degradation}} \quad (2.3.13)$$

- Develop a simple enough model that still captures all the underlying biological mechanisms and describes immune checkpoint inhibitor therapy.
 - Examine the effects of a single treatment to enhance the appreciation and understanding of a combined treatment.
-

Model Formulation

C = cancer cells

T = T-cells



Model Formulation

$$\frac{dC}{dt} = \underbrace{\lambda_C C \left(1 - \frac{C}{C_K}\right)}_{\text{net tumor growth}} - \underbrace{\eta CT}_{\text{killed by T cells}}$$

$$\frac{dT}{dt} = \left(\underbrace{\lambda_{TI_{12}} T_N \frac{I_{12}}{K_{I_{12}} + I_{12}}}_{\text{activation by IL-12}} + \underbrace{\lambda_{TI_2} T \frac{I_2}{K_{I_2} + I_2}}_{\text{stimulation by IL-2}} \right) \cdot \underbrace{\frac{1}{1 + \frac{Q}{K_{TQ}}}}_{\text{inhibition by PD-1-PD-L1}} - \underbrace{d_T T}_{\text{death}}$$

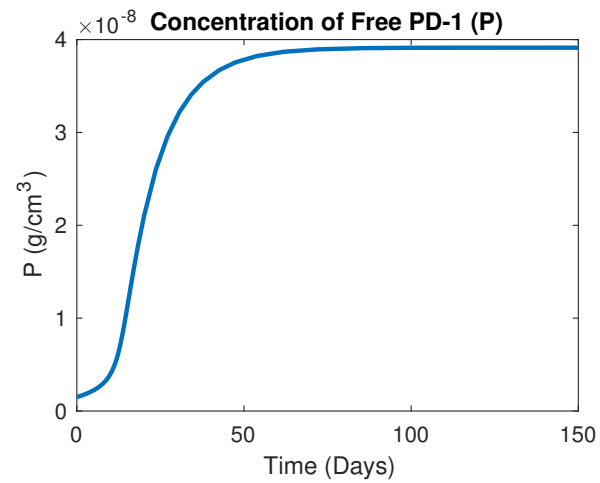
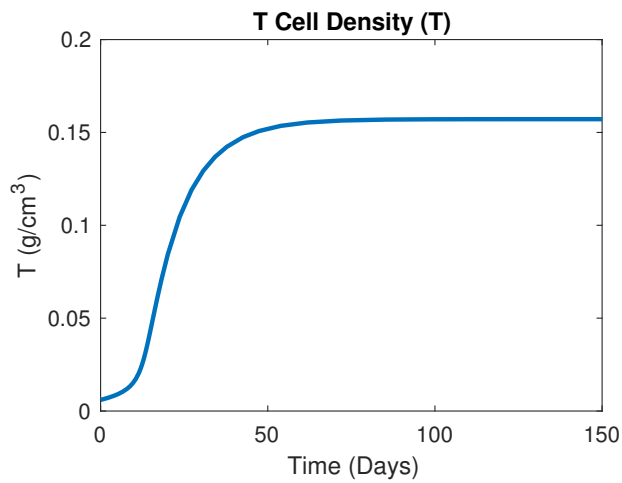
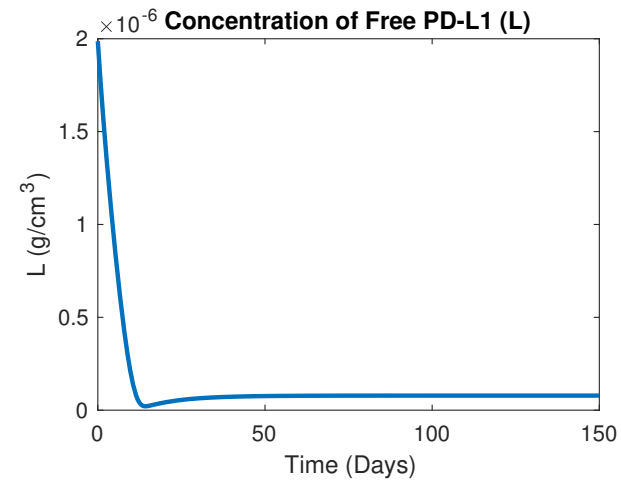
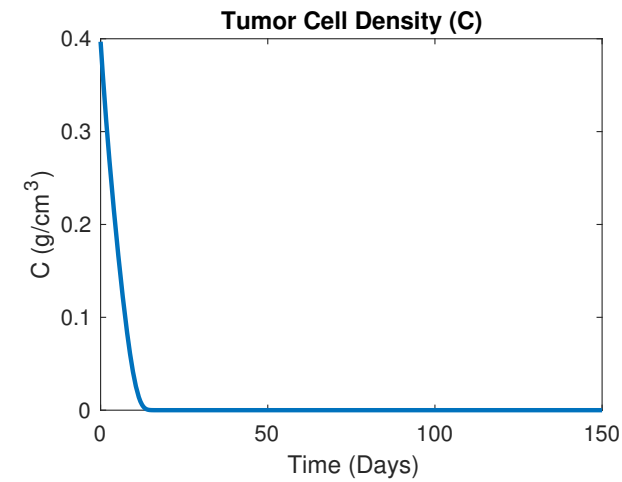
$$\frac{dA}{dt} = \underbrace{\gamma(t)}_{\text{effective level of anti-PD-1}} - \underbrace{\mu_{PA} PA}_{\text{depletion through blocking PD-1}} - \underbrace{d_A A}_{\text{natural degradation}}$$

$$Q = \sigma PL$$

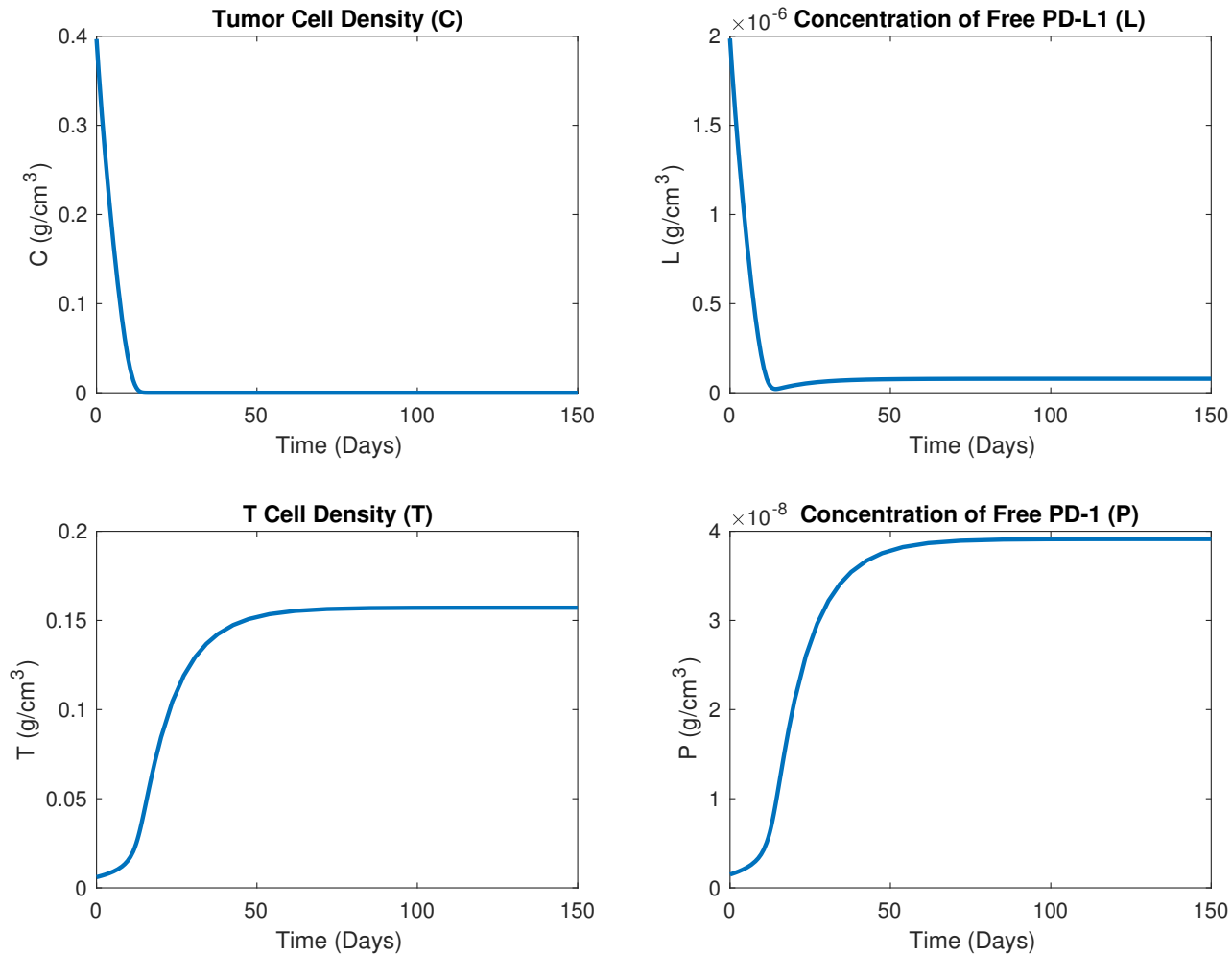
$$P = (\rho_p - \gamma A) T$$

$$L = \rho_L (T + \epsilon_C C)$$

Case 1: No Drug + Strong Immune System

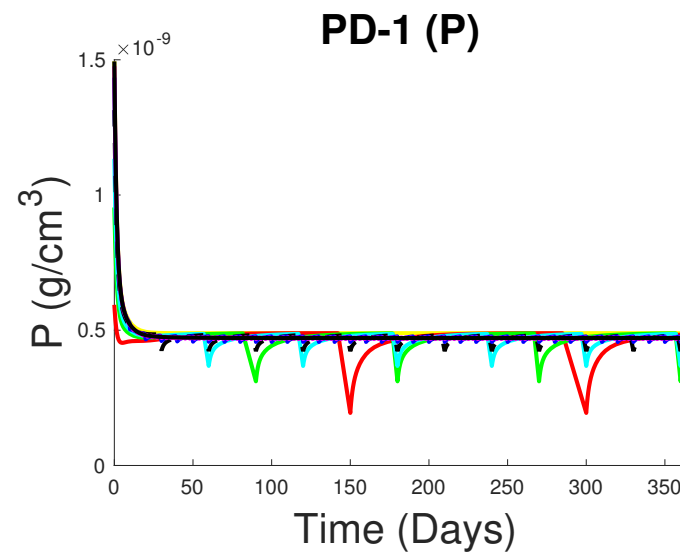
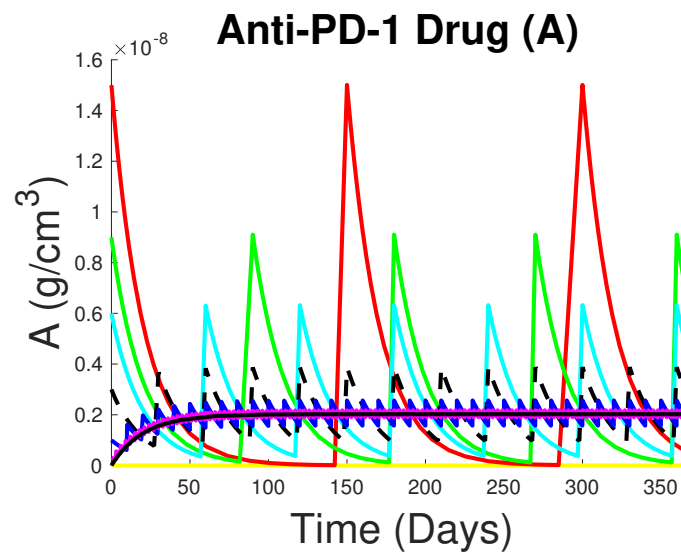
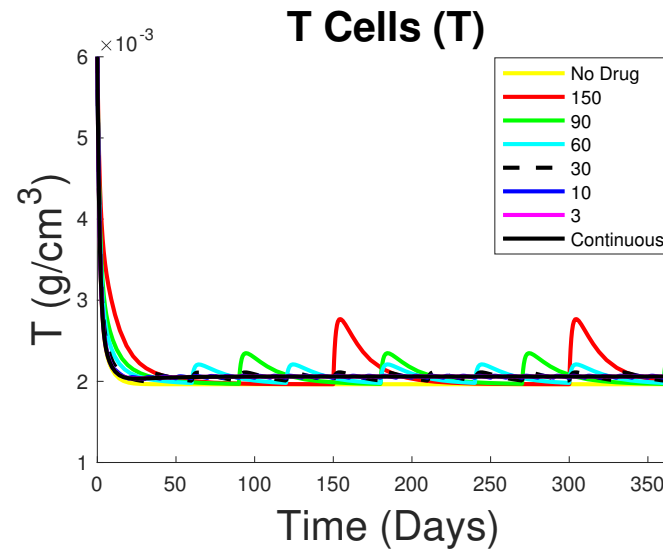
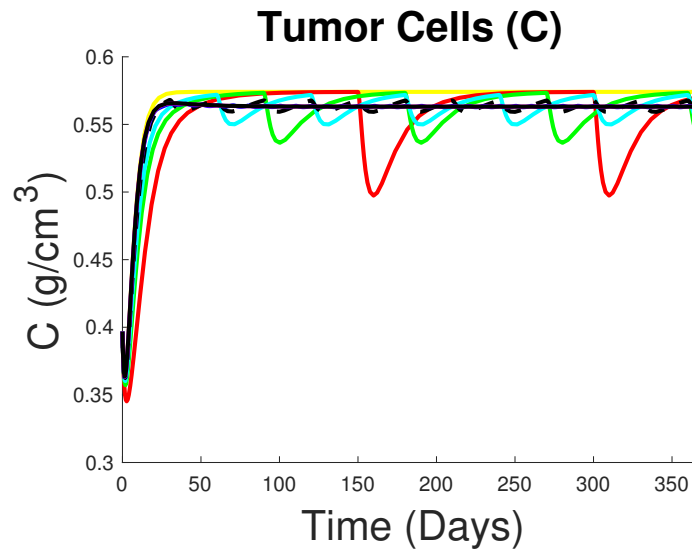


Case 1: No Drug + Strong Immune System

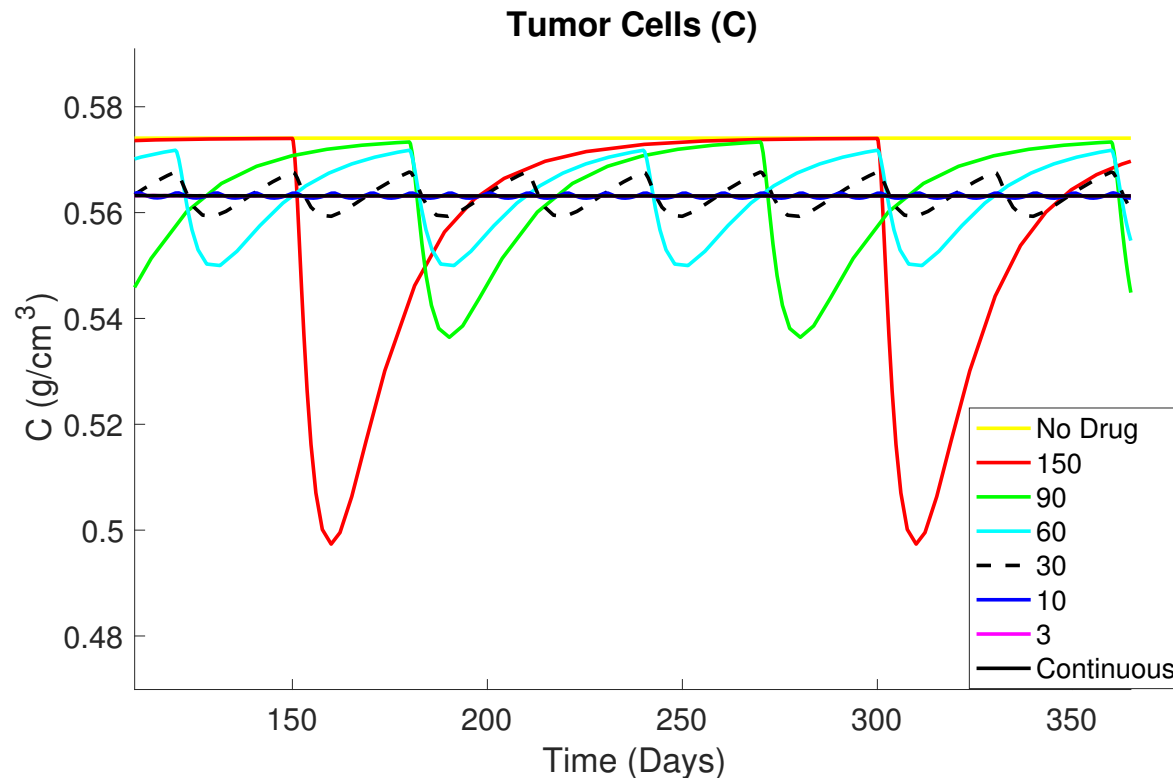


- People with a strong immune system have a chance to eradicate tumor.

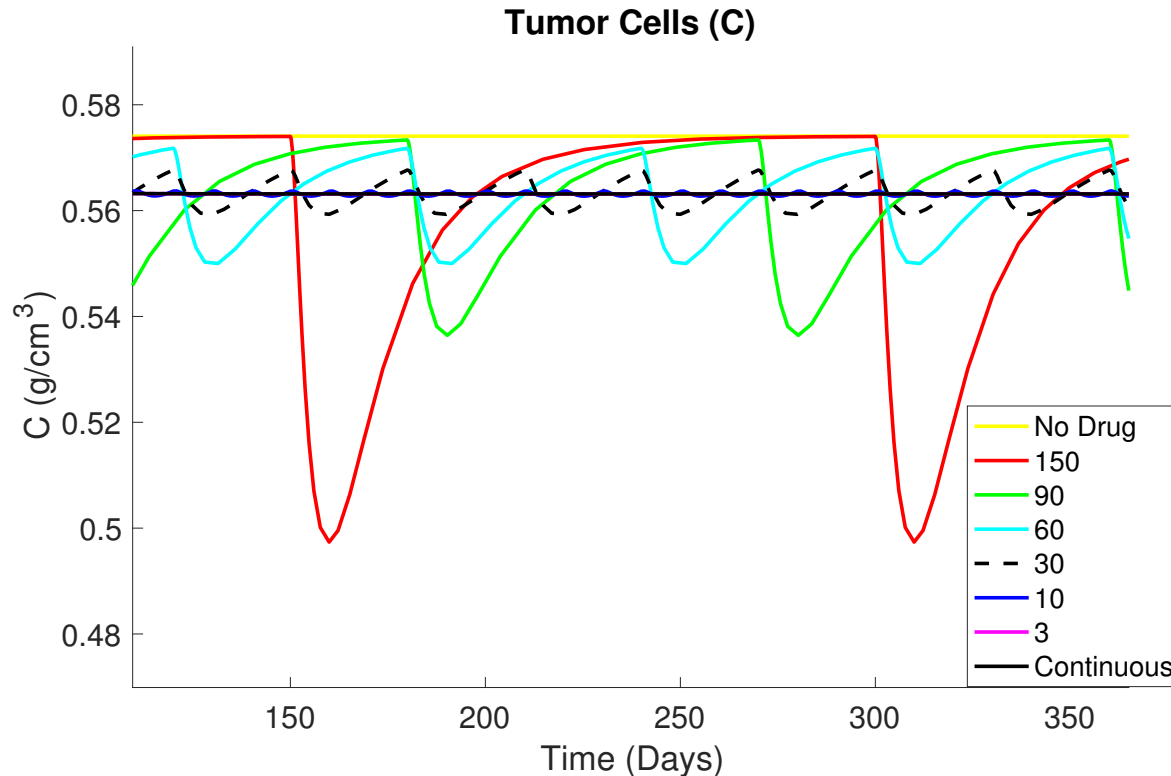
Case 2: Intermittent Treatment



Case 2: Intermittent Treatment: Close up

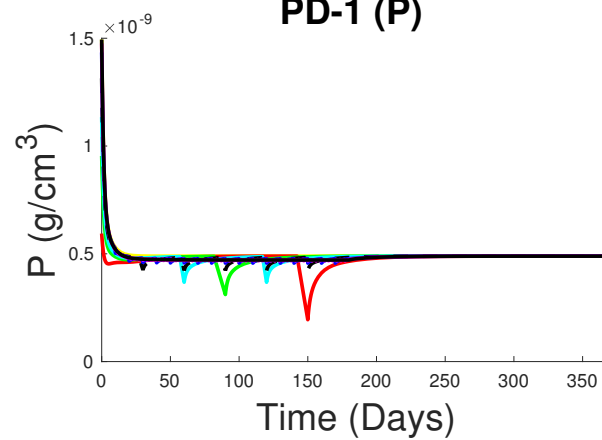
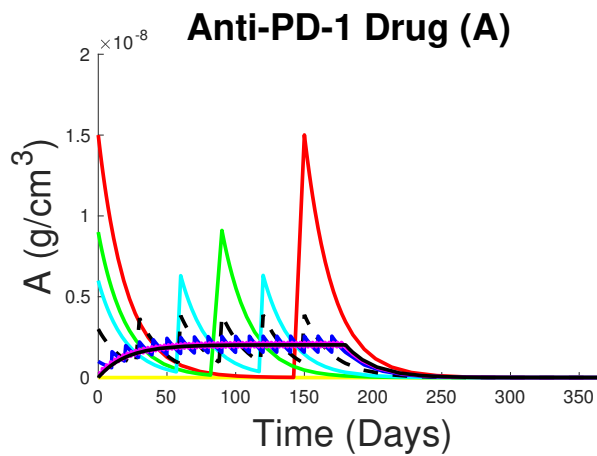
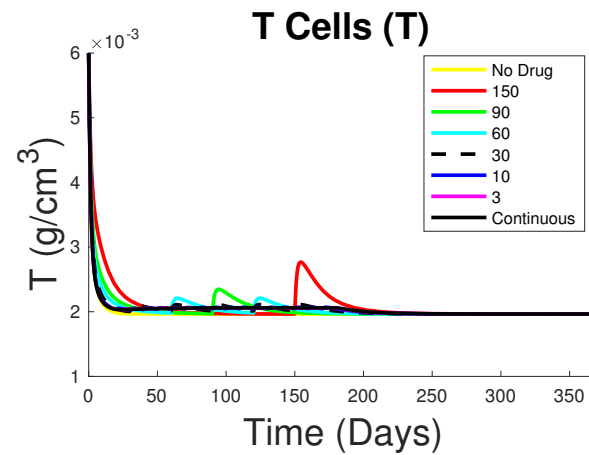
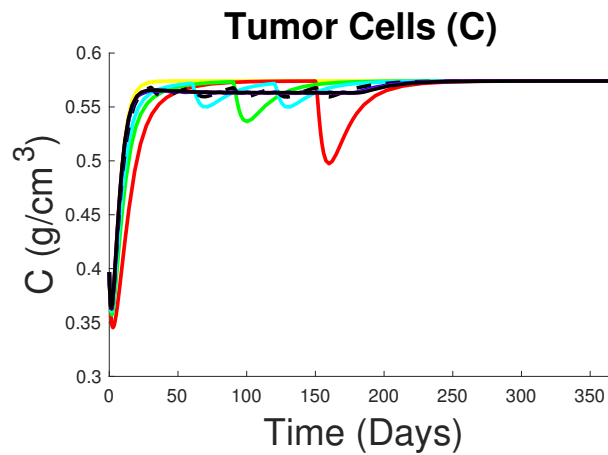


Case 2: Intermittent Treatment: Close up

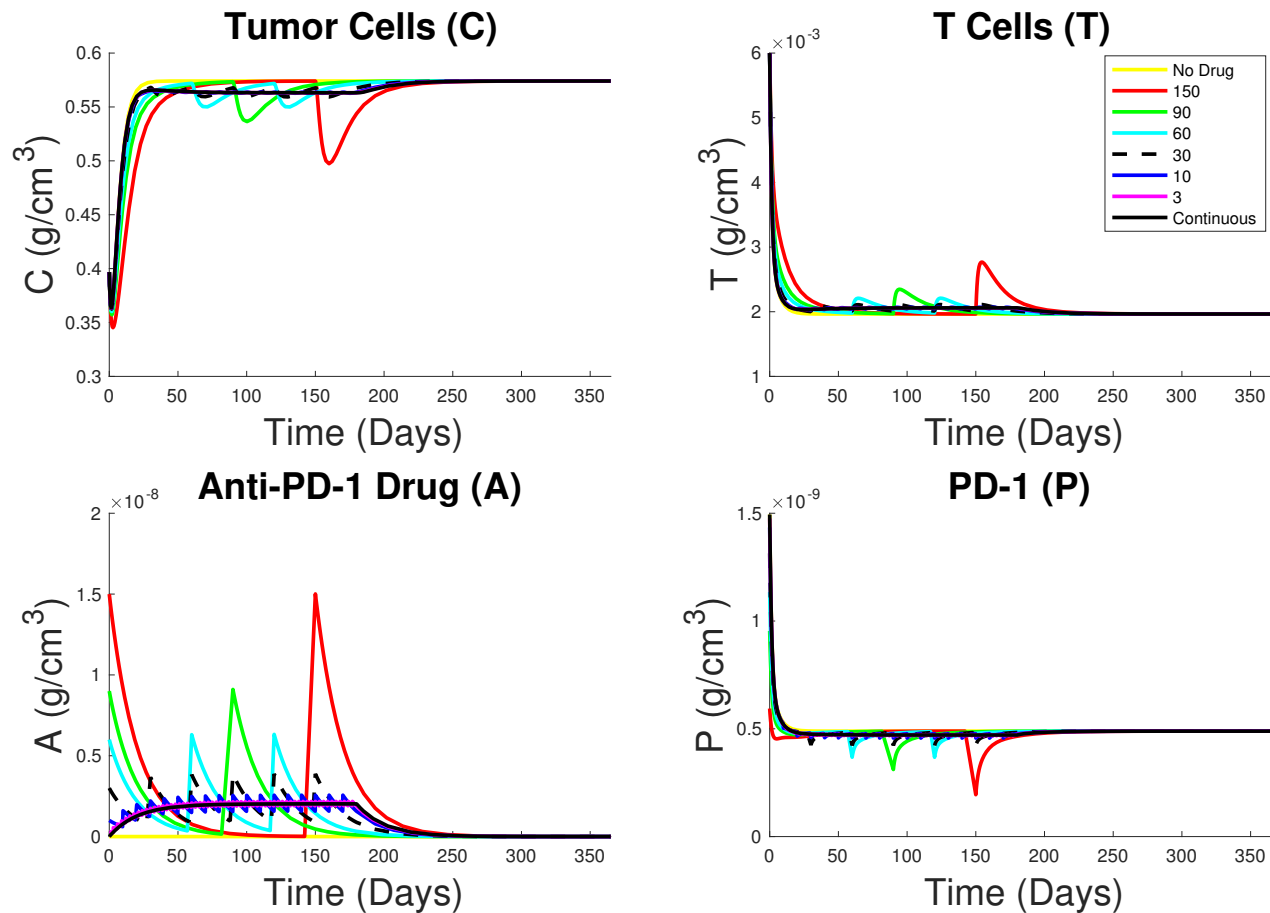


- More frequent treatments produce more effective results compared to less frequent.
- A continuous therapy offers the best control for the tumor cells.

Case 3: Switch on/off Treatment



Case 3: Switch on/off Treatment



- Once the treatment has ended, the density of the tumour cells and activated T cells eventually approach the same steady state as if no drug had ever been applied.

Conclusion for Project 1

- ➊ Cancers are more common and significant for patients with weakened immune systems.
- ➋ Continuous treatment is more preferable to intermittent treatment in this case.
- ➌ Upon intermittent treatment more frequent injections proved to have more effective results.
- ➍ Combining anti-PD-1 with an additional treatment is the most effective way to treat tumors.

Open Questions for Project 1

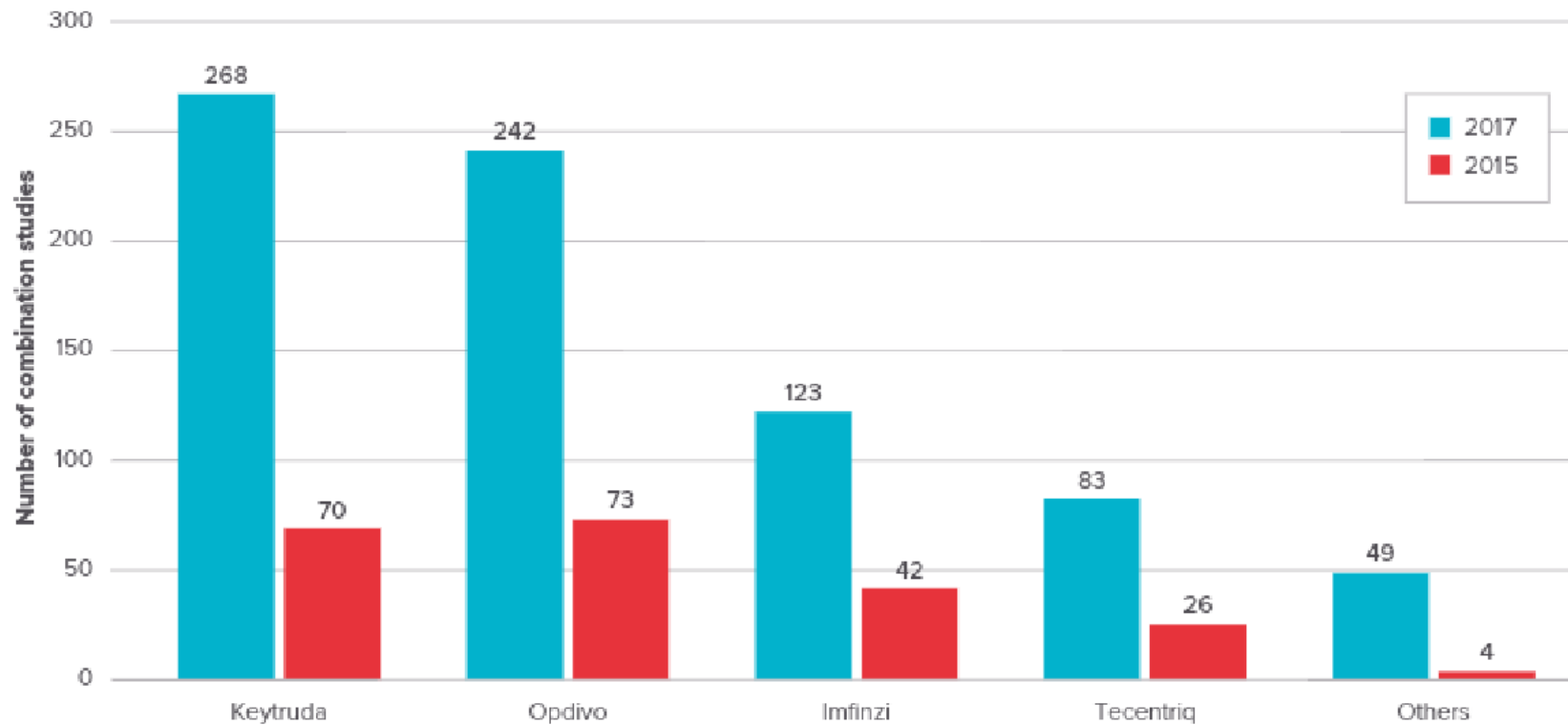
- 1 Connect the model to preclinical data (Project 2).
- 2 Adapt the model to investigate a combination type of treatment (Project 2).
- 3 Perform mathematical analysis on the full model (Shi *et al.* (2020))
- 4 Examine the effects of treatment resistance through the incorporation of two competing cancer species (sensitive/insensitive).

¹Shi, S., J. Huang and Y. Kuang, “Global dynamics in a tumor-immune model with an immune checkpoint inhibitor.” DCDS-B in review (2020).

Motivation

Number of Anti-PD-1/PD-L1 MAb combination studies 2015 vs. 2017

Source: Evaluate Ltd.* May 2017



- Dramatic increase in the number of clinical trials between 2015 and 2017.

Research Articles

Tumour-immune dynamics with an immune checkpoint inhibitor

Elpiniki Nikolopoulou, Lauren R. Johnson, Duane Harris, John D. Nagy, Edward C. Stites & Yang Kuang

Pages 5137-5159 | Received 18 Dec 2017, Accepted 08 Feb 2018, Published online: 09 Mar 2018

Download citation

https://doi.org/10.1080/23737867.2018.1440978

Check for updates

Cancer Therapy: Preclinical

Combination Therapy with NHS-muIL12 and Avelumab (anti-PD-L1) Enhances Antitumor Efficacy in Preclinical Cancer Models

Chunxiao Xu, Yanping Zhang, P. Alexander Rofe, Vivian M. Hernández, Wilson Guzman, Giorgio Kradjian, Bo Marelli, Guozhong Qin, Jin Qi, Hong Wang, Huakui Yu, Robert Tighe, Kin-Ming Lo, Jessie M. English, Laszlo Radvanyi, and Yan Lan

DOI: 10.1158/1078-0432.CCR-17-0483 Published October 2017

Check for updates

Combination therapy of cancer with cancer vaccine and immune checkpoint inhibitors: A mathematical model

Xiulan Lai, Avner Friedman

Published: May 25, 2017 • https://doi.org/10.1371/journal.pone.0178479

Notation	Description	units
D	density of DCs	g/cm^3
T_1	density of activated CD4^+ T cells	g/cm^3
T_8	density of activated CD8^+ T cells	g/cm^3
C	density of cancer cells	g/cm^3
N_C	density of necrotic cancer cells	g/cm^3
H	HMGB-1 concentration	g/cm^3
G	GM-CSF concentration	g/cm^3
I_{12}	IL-12 concentration	g/cm^3
I_2	IL-2 concentration	g/cm^3
P	PD-1 concentration	g/cm^3
L	PD-L1 concentration	g/cm^3
Q	PD-1-PD-L1 concentration	g/cm^3
A	anti-PD-1 concentration	g/cm^3

https://doi.org/10.1371/journal.pone.0178479.t001

Formulation of Mathematical Model

Variable	Meaning	Unit
V	tumor cell volume	mm^3
T	volume of activated T cells	mm^3

$$\begin{aligned}\frac{dV}{dt} &= Vg(V) - p(V)T \\ \frac{dT}{dt} &= \delta F(V, T) - d_T T\end{aligned}$$

- 1 The tumor growth rate $g(V)$ is a continuously differentiable function and there exists a $K > 0$ such that $g(V) > 0$ when $V \in (0, K)$ and $g(V) < 0$ for $V > K$.
- 2 The kill rate of the tumor cells $p(V)$ is an increasing function of the tumor volume V such that $p(0) = 0$.
- 3 The T cell activation function $F(V, T)$ is a positive and decreasing function of both variables.

Equilibria and Stability

There are two unique equilibria:

- $E_0^* = (0, T_0^*)$ tumor-free
- $E^* = (V^*, T^*)$ tumorous

Let $H(V) = \frac{Vg(V)}{p(V)}$

Theorem

E_0^* is globally attractive with respect to positive solutions if $H'(V) < 0$ for $V > 0$ and $\delta F(V, H(V)) - d_T H(V)$ has no positive solution.

Proposition 3.4.5

$E^* = (V^*, T^*)$ is stable if $H'(V^*) < 0$ and

$$H'(V^*) \left[\delta \frac{\partial}{\partial T} F(V^*, T^*) - d_T \right] + \delta \frac{\partial}{\partial V} F(V^*, T^*) > 0$$

Logistic Growth Dynamics

$$\begin{aligned}\frac{dV}{dt} &= Vg(V) - p(V)T \\ \frac{dT}{dt} &= \delta F(V, T) - d_T T\end{aligned}$$

where,

$$g(V) = r\left(1 - \frac{V}{V_K}\right), p(V) = \eta V$$

Theorem

The following are true:

- *If $r < \eta T_0^*$ and no tumorous equilibrium exists, then the tumor-free equilibrium E_0^* of the system is globally asymptotically stable.*
- *If $\frac{\eta \epsilon_V V_K}{r} < 1$ and $f(\frac{r}{\eta}) < 0$ then the tumorous steady state E of the system is globally asymptotically stable.*

Exponential Growth Dynamics

$$\begin{aligned}\frac{dV}{dt} &= Vg(V) - p(V)T \\ \frac{dT}{dt} &= \delta F(V, T) - d_T T\end{aligned}$$

where,

$$g(V) = r, p(V) = \eta V$$

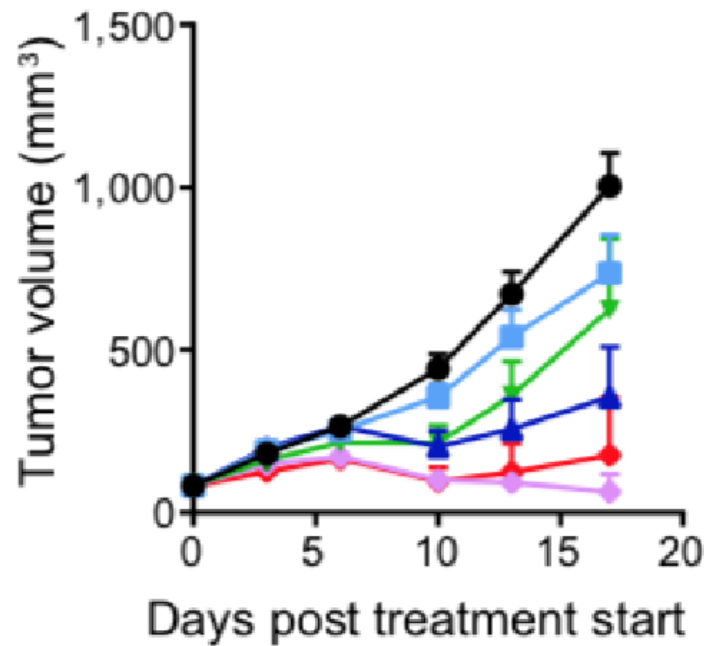
Corollary (3.4.12)

E_0^* is locally asymptotically stable if $r < \eta T_0^*$.

Corollary (3.4.13)

E^* is a saddle point.

Experimental Mice Data in Xu et al. (2017)



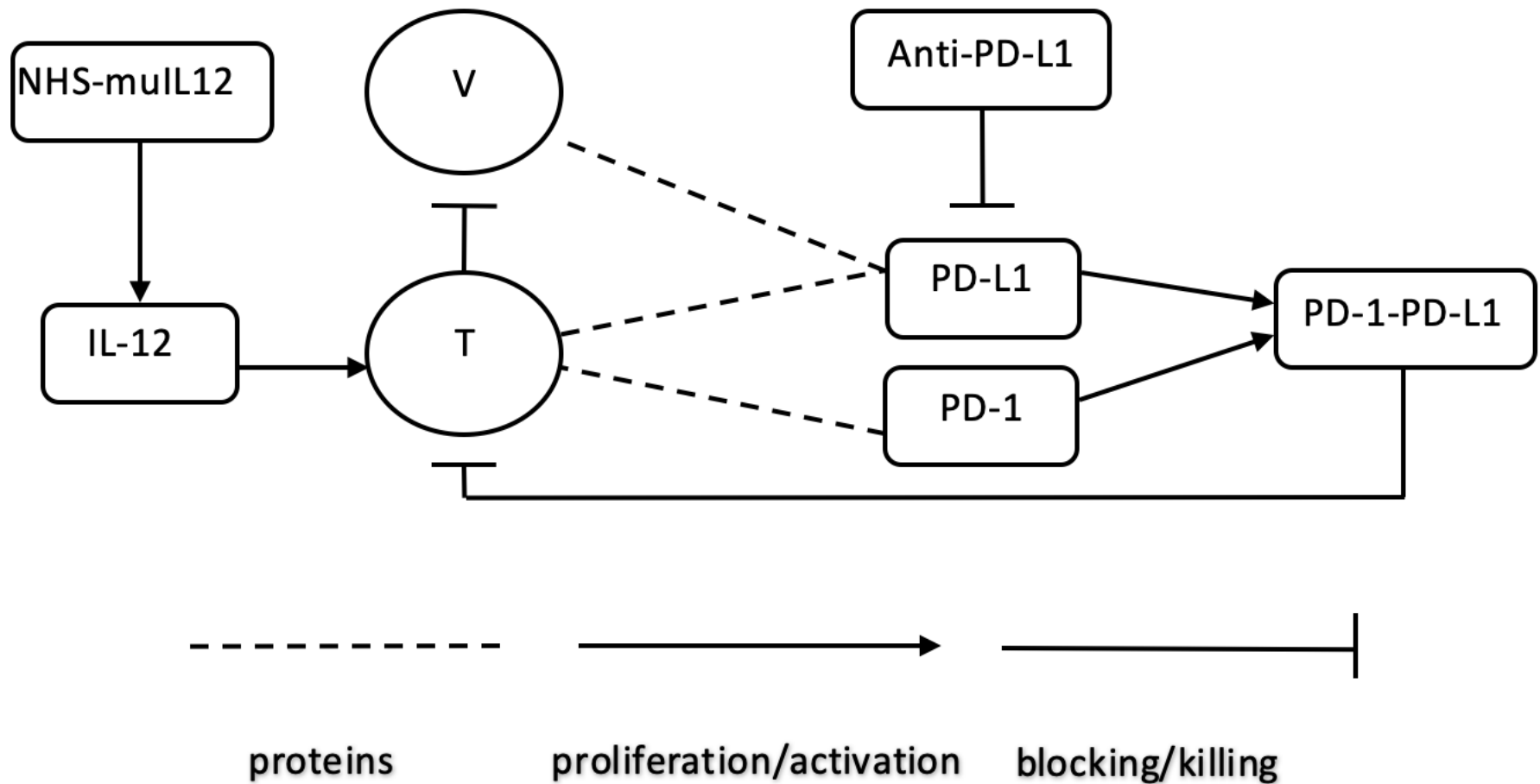
- No drug
- NHS-muIL12 (2 µg)
- NHS-muIL12 (10 µg)
- Avelumab (200 µg)
- NHS-muIL12 (2 µg) + Avelumab (200 µg)
- NHS-muIL12 (10 µg) + Avelumab (200 µg)

- Combination therapy enhanced antitumor efficacy compared to monotherapy.

Model Flow-Chart

V = volume of tumor cells

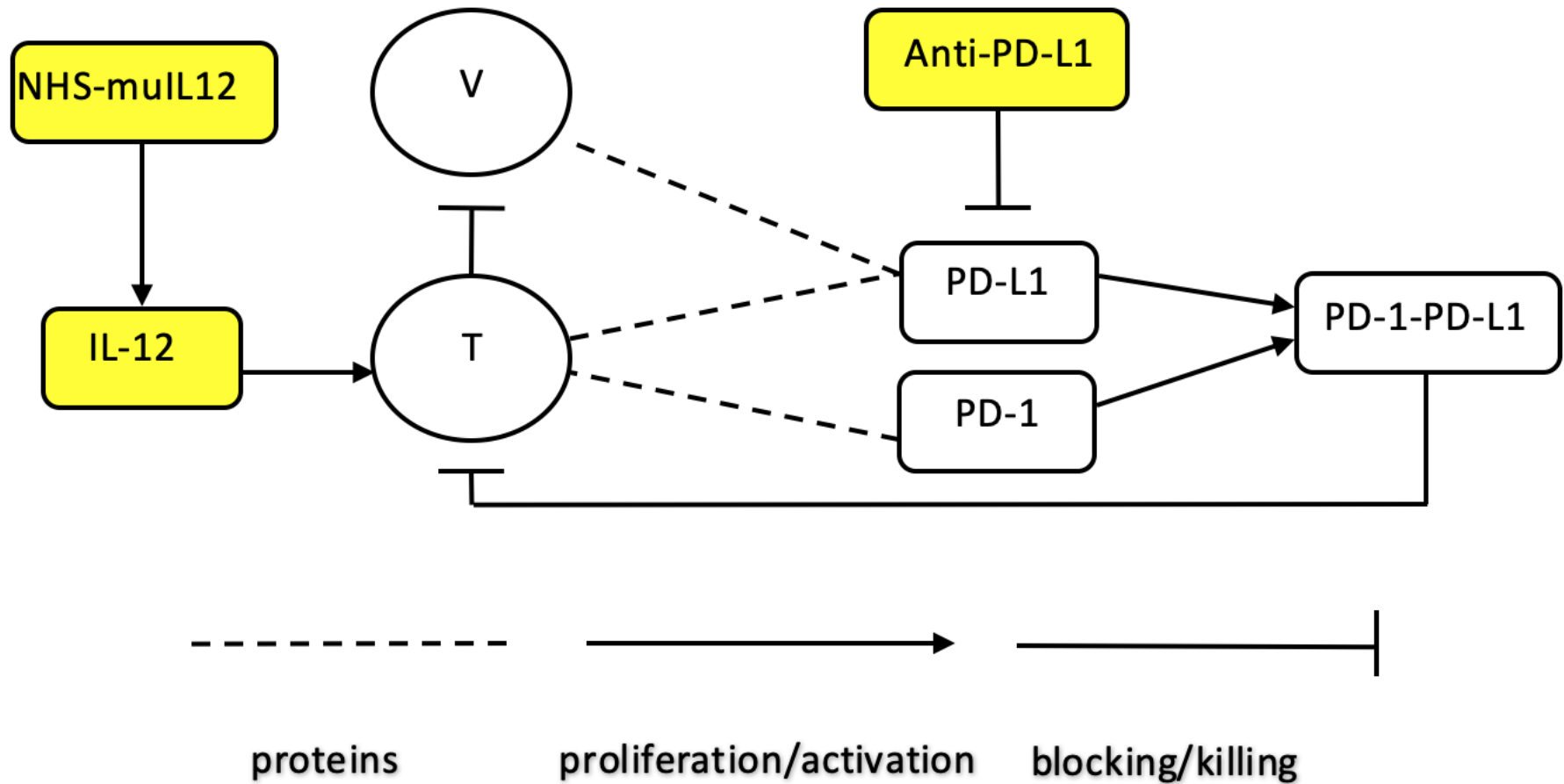
T = volume of T-cells



Model Flow-Chart

V = volume of tumor cells

T = volume of T-cells



Model Formulation

$$\frac{dV}{dt} = \underbrace{rV}_{\text{net tumor growth}} - \underbrace{\eta VT}_{\text{killed by T cells}}$$

$$\frac{dT}{dt} = \left(\underbrace{\delta}_{\text{source}} + \underbrace{\lambda_{TI_{12}} T \frac{c_2 A_2}{K_{A_2} + c_2 A_2}}_{\text{stimulation by IL-12}} \right) \cdot \underbrace{\frac{1}{1 + \frac{Q(V, T, A_1)}{K_{TQ}}}}_{\text{inhibition by PD-1-PD-L1}} - \underbrace{d_T T}_{\text{death}}$$

$$\frac{dA_1}{dt} = \underbrace{\gamma_1(t)}_{\text{infusion rate of avelumab}} - \underbrace{d_{A_1} A_1}_{\text{natural degradation}}$$

$$\frac{dA_2}{dt} = \underbrace{\gamma_2(t)}_{\text{infusion rate of NHS-muIL12}} - \underbrace{d_{A_2} A_2}_{\text{natural degradation}}$$

$$Q = \sigma \rho_P \rho_L T (T + \epsilon_v V) \left(1 - \frac{A_1}{A_1 + K_{A_1}} \right)$$

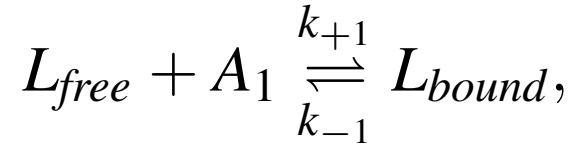
Derivation of Q (PD-1-PD-L1 Complex)

$$L_{total} = L_{free} + L_{bound}$$

$$L_{free} = \rho_L(T + \epsilon_v V) - L_{bound}$$

$$Q = \sigma P L_{free} = \sigma \rho_p T (\rho_L(T + \epsilon_v V) - L_{bound}) \quad (1)$$

Next, we consider the reaction scheme:

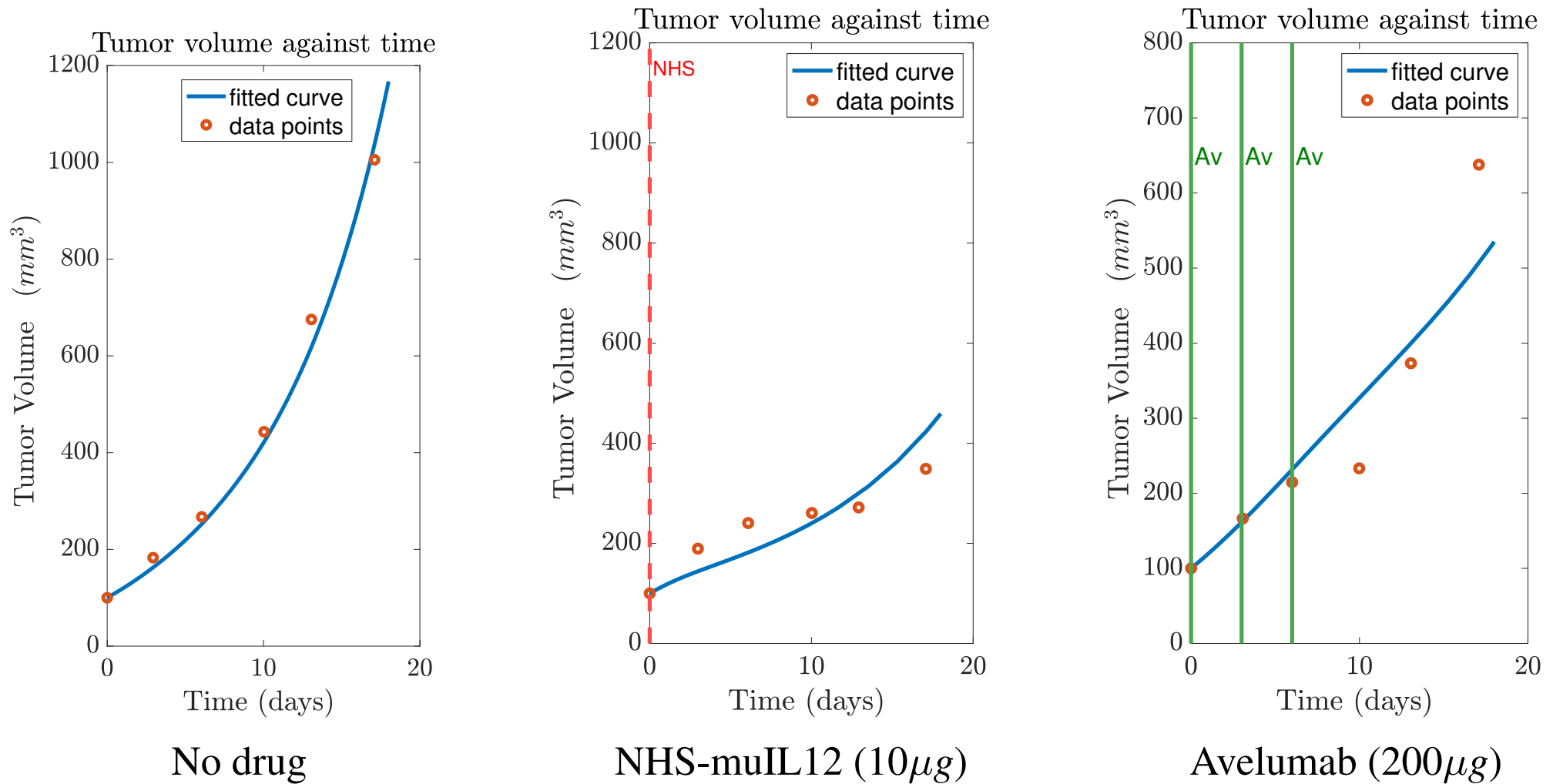


$$L_{bound} = \frac{A_1}{A_1 + K_{A_1}} (\rho_L(T + \epsilon_v V)) \quad (2)$$

By substituting equation (2) into equation (1), we derive the following expression for Q ,

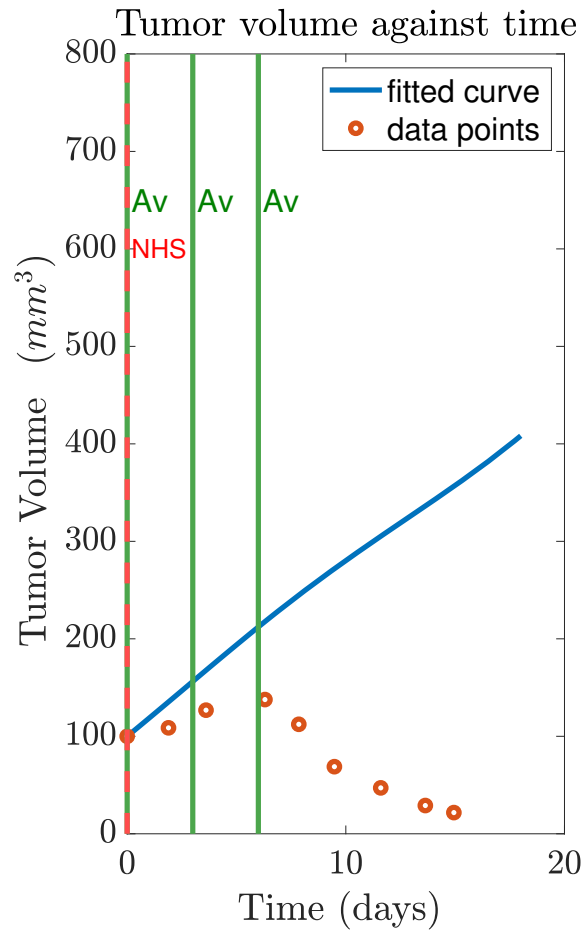
$$Q = \sigma \rho_P \rho_L T (T + \epsilon_v V) \left(1 - \frac{A_1}{A_1 + K_{A_1}} \right), \text{ with } \sigma = \alpha_{PL}/d_Q.$$

Submodel Fits to Data: Monotherapy Treatment

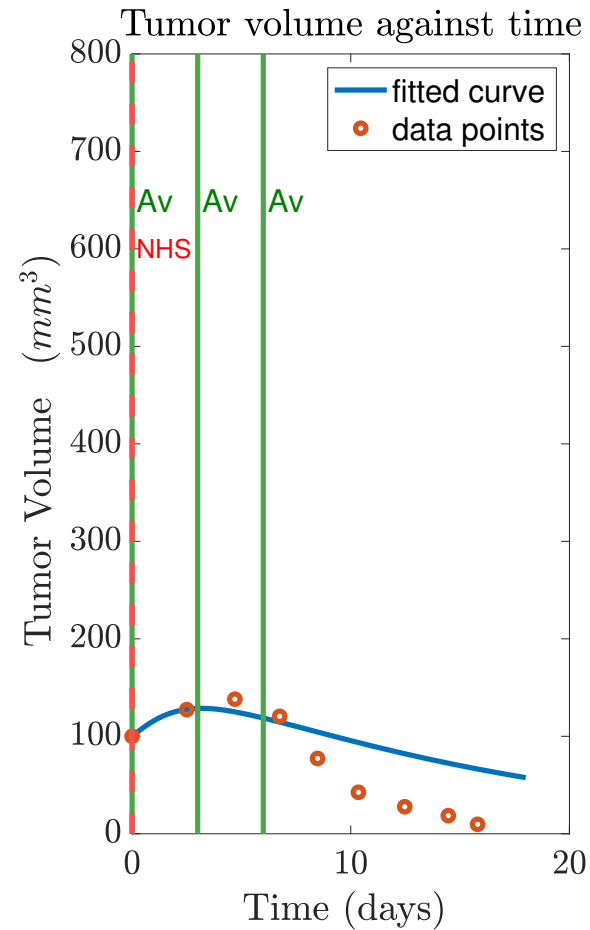


- Relatively good fits for the monotherapy case

Predictions: Combination Treatment



Av ($200\mu g$) + NHS ($2\mu g$)



Av ($200\mu g$) + NHS ($10\mu g$)

- Not qualitatively as good fits

Synergy Between Avelumab and NHS-muIL12 (Full System)

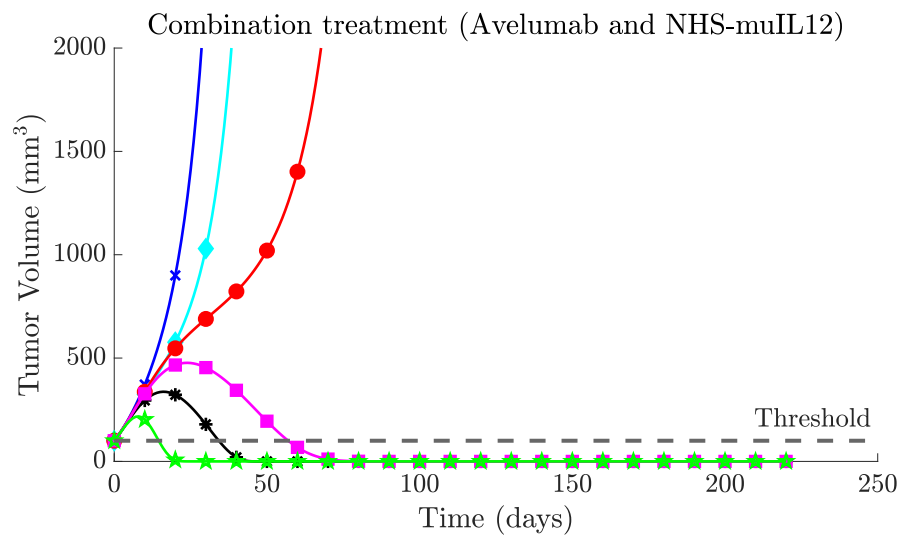
γ_1 = Avelumab

γ_2 = NHS-muIL12

Synergy Between Avelumab and NHS-muIL12 (Full System)

γ_1 = Avelumab

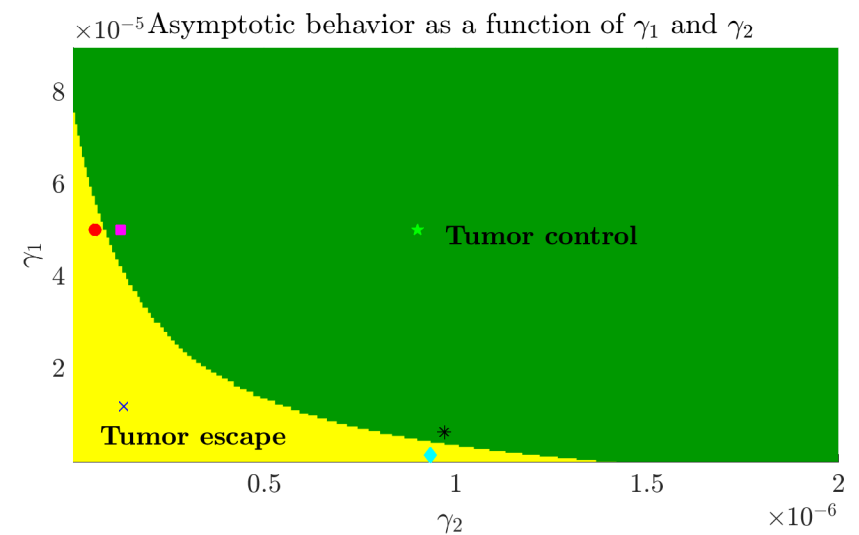
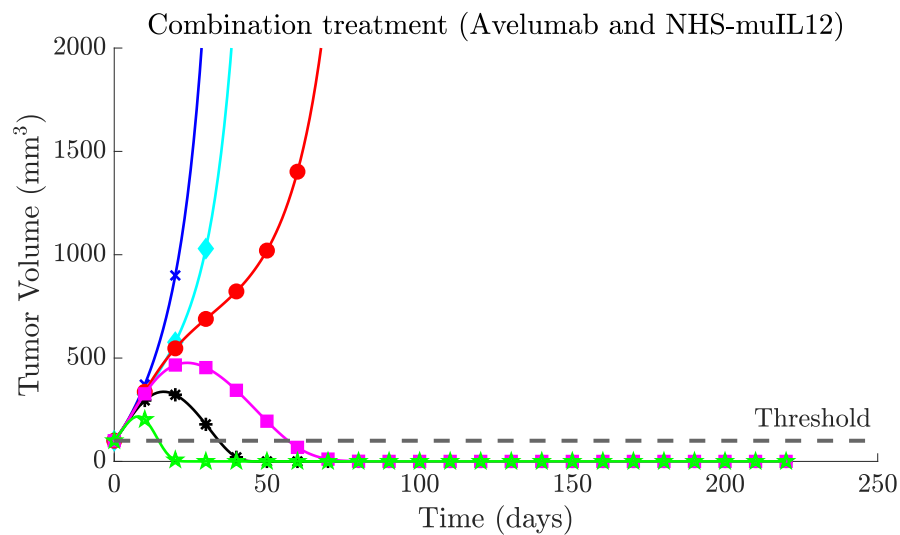
γ_2 = NHS-muIL12



Synergy Between Avelumab and NHS-muIL12 (Full System)

γ_1 = Avelumab

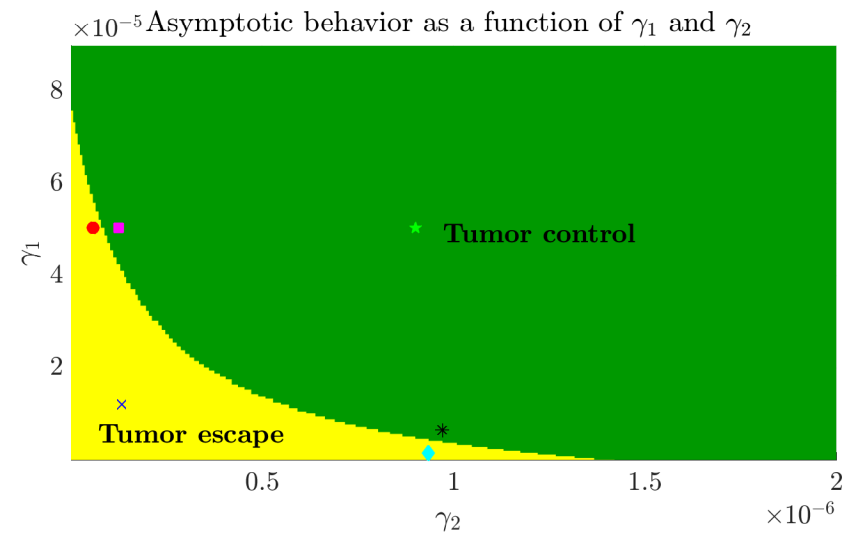
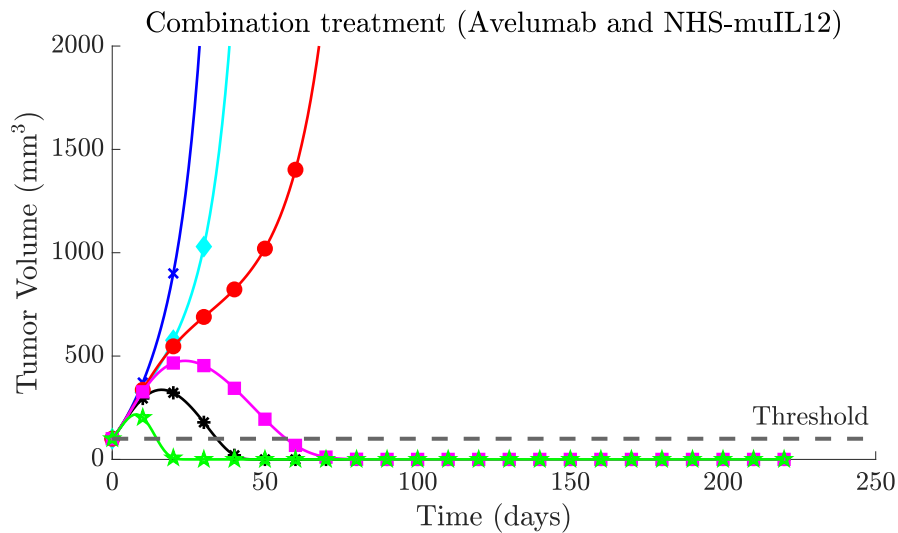
γ_2 = NHS-muIL12



Synergy Between Avelumab and NHS-muIL12 (Full System)

γ_1 = Avelumab

γ_2 = NHS-muIL12



- About a third of the two drugs in combination required compared to monotherapy.

Limiting System

Using a quasi-state approximation: $A_1 = \frac{\gamma_1}{d_{A1}}$ and $A_2 = \frac{\gamma_2}{d_{A2}}$

$$\frac{dV}{dt} = rV - \eta VT,$$

$$\frac{dT}{dt} = \left(\delta + \lambda_{TI_{12}} TM \right) F(V, T) - d_T T$$

where,

$$M = \frac{c_2 \gamma_2}{d_{A_2} K_{A_2} + c_2 \gamma_2},$$

$$N = \frac{c_1 \gamma_1}{d_{A_1} K_{A_1} + c_1 \gamma_1},$$

$$Q = \sigma \rho_p \rho_l T (T + \epsilon_v V) (1 - N),$$

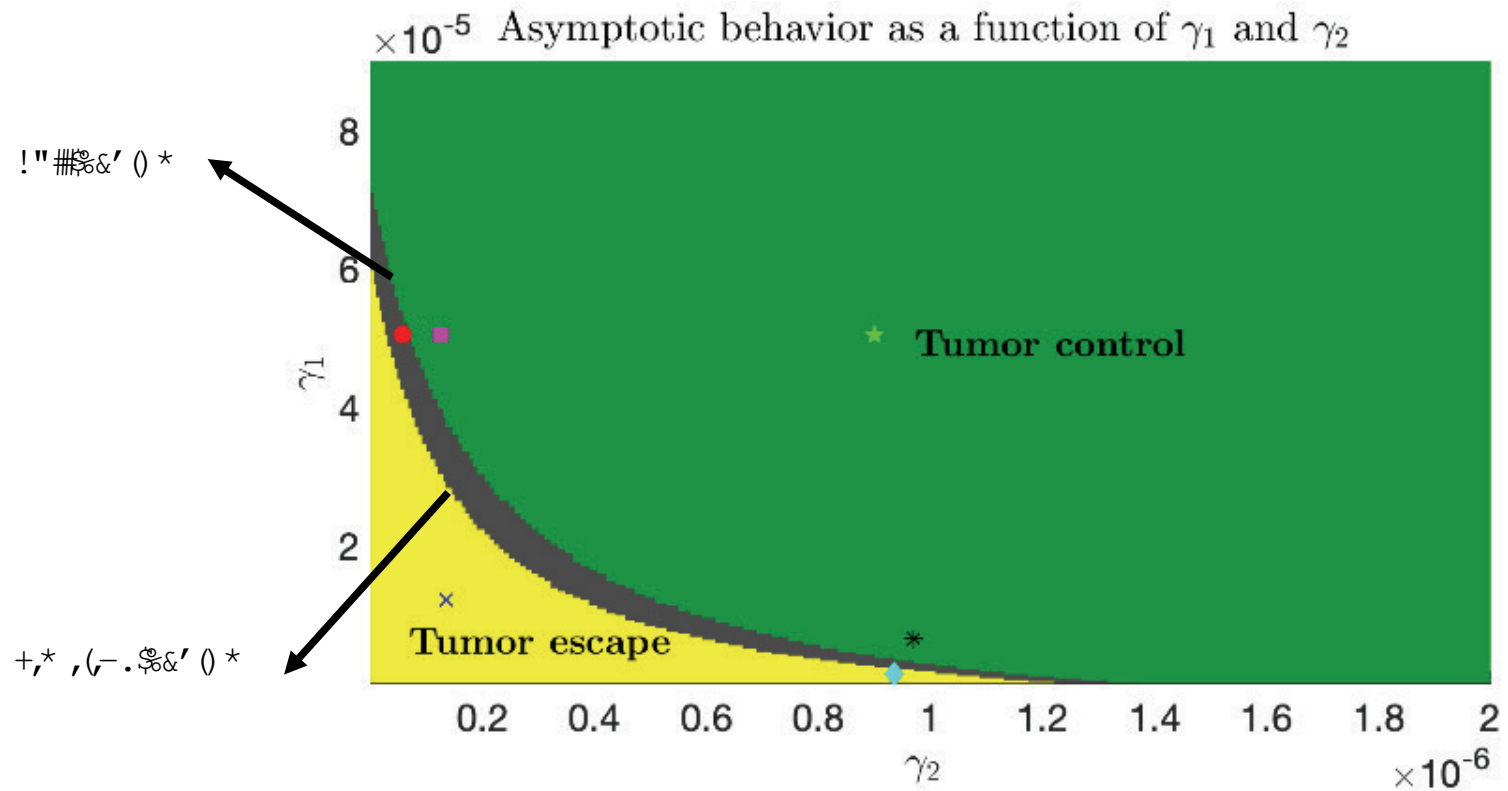
$$F(V, T) = \frac{1}{1 + \alpha' T (T + \epsilon_v V)},$$

$$\alpha' = \frac{\sigma \rho_p \rho_l}{K_{TQ}} (1 - N), \quad \text{with } N < 1.$$

Full System vs Limiting System

γ_1 = Avelumab

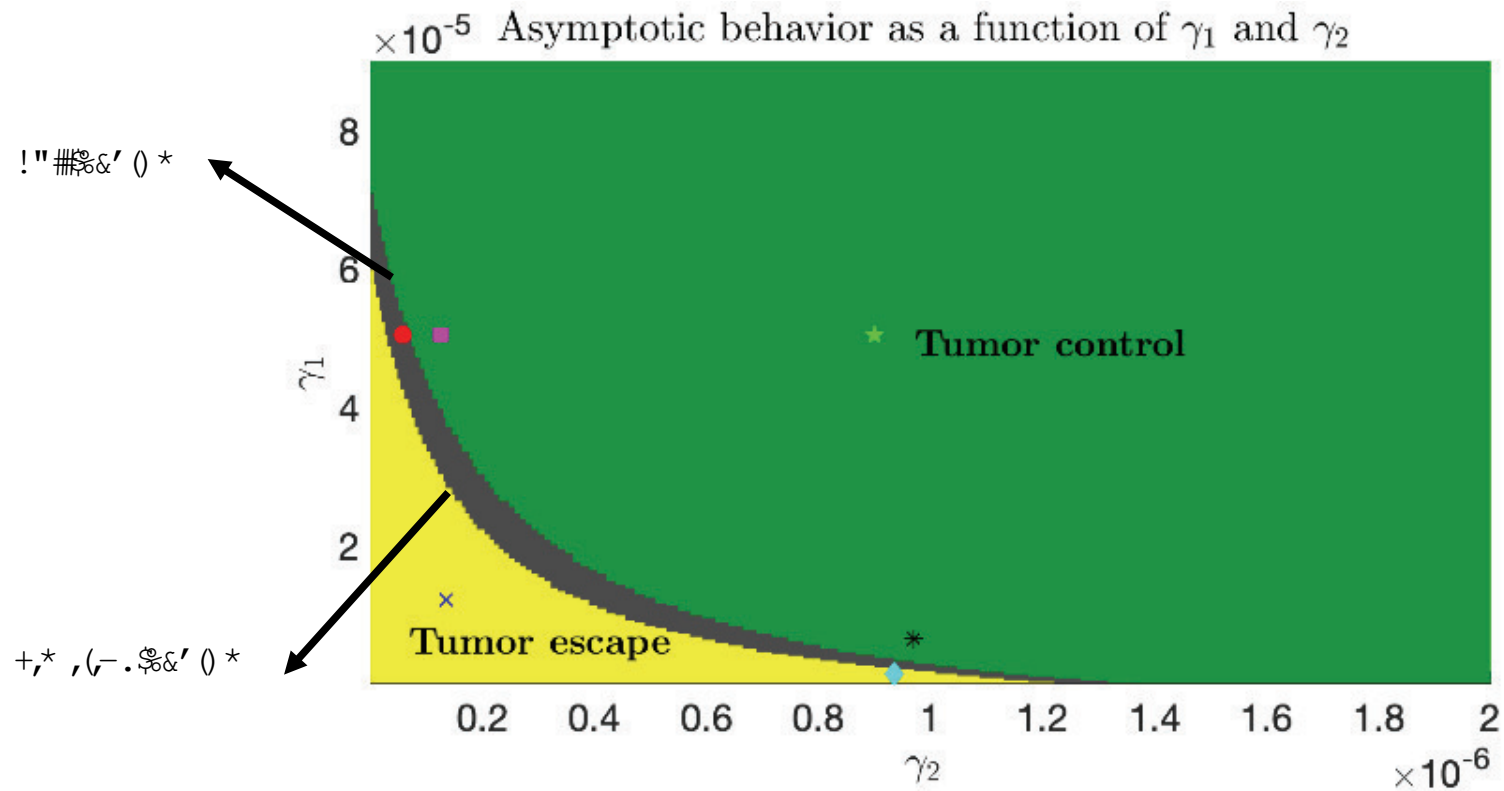
γ_2 = NHS-muIL12



Full System vs Limiting System

γ_1 = Avelumab

γ_2 = NHS-muIL12



- Qualitative behavior of the systems is comparable.

Conclusion

- ① Developed a simple biologically meaningful system that models the tumor volume behavior given the mice data.
- ② Able to fit well the submodels of the full model to the monotherapy cases.
- ③ Model predictions indicated that the dual therapy at lower doses of NHS-muIL12 well is not well described. However, the model does make qualitatively good predictions at higher NHS-muIL12 doses.
- ④ The treatment regimen of continuous administration used for both the full and limiting system suggested similar qualitative behavior.
- ⑤ The two drugs act synergistically, such that, compared to monotherapy, only about one-third the dose of both drugs is required in combination for tumor control.

Back to Elpi's Original Model

Bruce Pell

Original Model

$$\left\{ \begin{array}{l} \frac{dV}{dt} = \underbrace{rV}_{\text{net tumor growth}} - \underbrace{\eta VT}_{\text{killed by T cells}}, \\ \frac{dT}{dt} = \underbrace{\delta F(V, T, A_1, A_2)}_{\text{T cell activation}} - \underbrace{d_T T}_{\text{death}}, \\ \frac{dA_1}{dt} = \underbrace{\gamma_1(t)}_{\text{infusion rate of avelumab}} - \underbrace{d_{A_1} A_1}_{\text{natural degradation}}, \\ \frac{dA_2}{dt} = \underbrace{\gamma_2(t)}_{\text{infusion rate of NHS-muIL12}} - \underbrace{d_{A_2} A_2}_{\text{natural degradation}}. \end{array} \right.$$

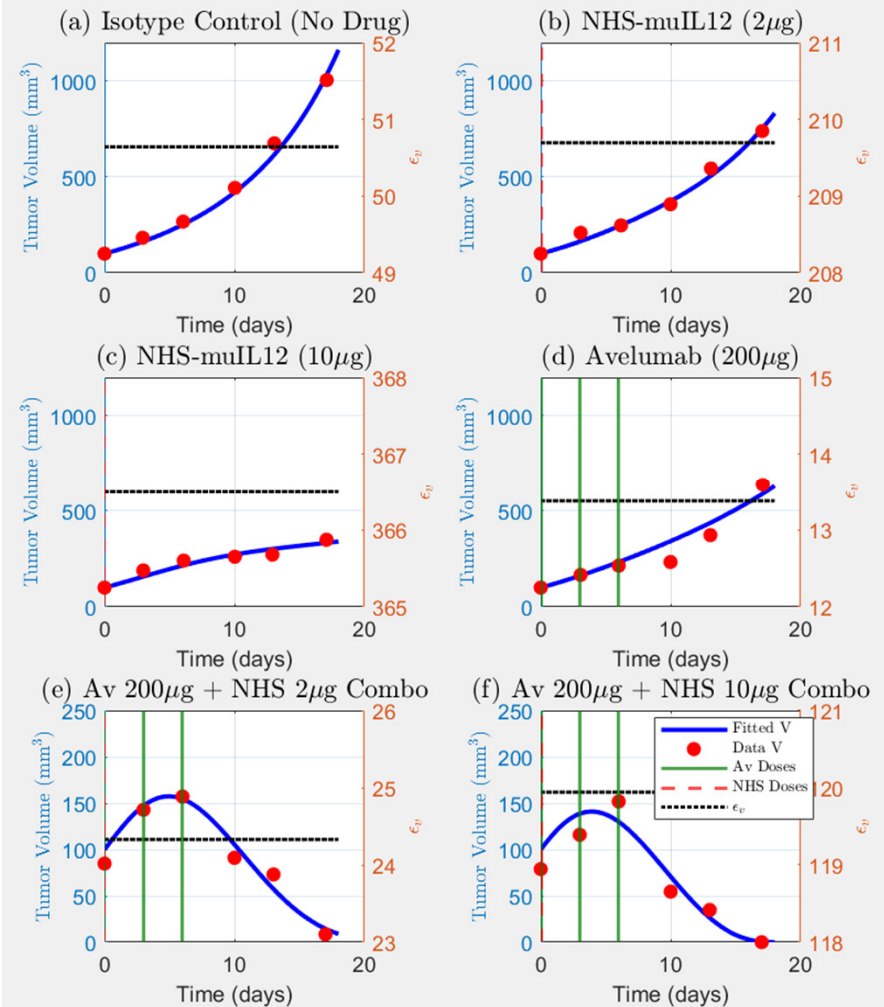
$$F = \left(1 + \frac{\lambda_{T12} T \cdot c_2 A_2}{K_{A_2} + c_2 A_2} \right) \cdot \frac{1}{1 + Q(V, T, A_1)/K_{TQ}}$$

$$Q(V, T, A_1) = \alpha' T (T + \epsilon_v V) (1 - \phi(A_1)) \quad \text{with} \quad \phi(A_1) = \frac{c_1 A_1}{c_1 A_1 + K_{A_1}}.$$

Elpi's Original Model

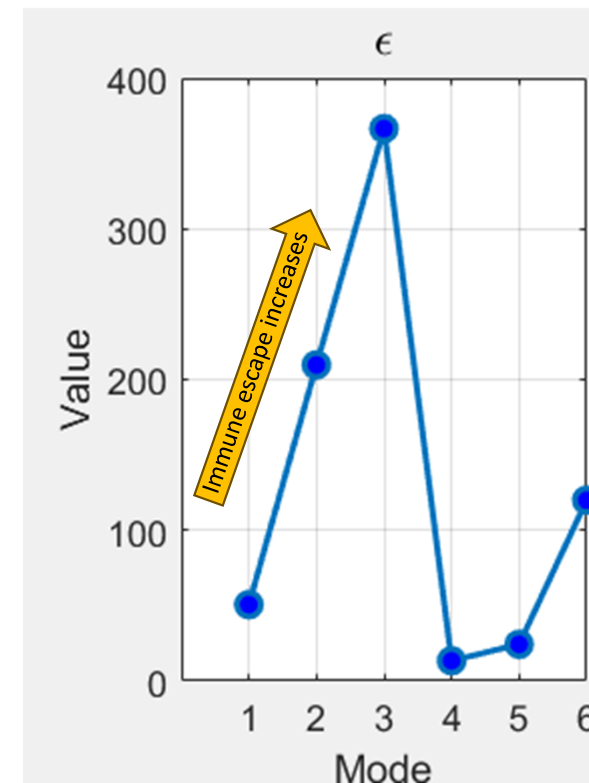
- Constant epsilon, but fitted for each mode. Fits are very nice!
- Slight changes to her original parameters:
 - Incorporated the 3 new parameter values suggested earlier by Aigerim.
 - Set K_{A1} and K_{A2} to the estimated values that Elpi derived from literature, but decided not to use.
 - I let epsilon range from 1 to 400 in the fitting process.

4-ODE Model Individual Fits (ϵ_v)



Epsilon across treatments: Adaptive Response

- **Observation:** All other parameters being fixed, epsilon increases with NHS-muLL12 treatment (mode 2 and 3) relative to the no drug case.
- **Proposed Mechanism:** Tumor is upregulating PD-L1 to counter the boosted immune system (T-cells) from the NHS-muLL12 treatment. More PD-L1 allows for more PD-1-PD-L1 complex, the complex that sends the signal to “switch off” the T-cells ability to kill.
- **Avelumab:** The introduction of Avelumab which is anti PD-L1 prevents the formation of the complex PD-1-PD-L1, by binding to PD-L1 in the tumor surface, thus reducing epsilon. Perhaps, epsilon should be thought of as proportion of *active/functional* PD-L1 from the tumor surface.
- **Combination:** Mode 5 and 6, show that NHS-muLL12 is again stimulating the tumor to upregulate PD-L1 to counter the immune system.

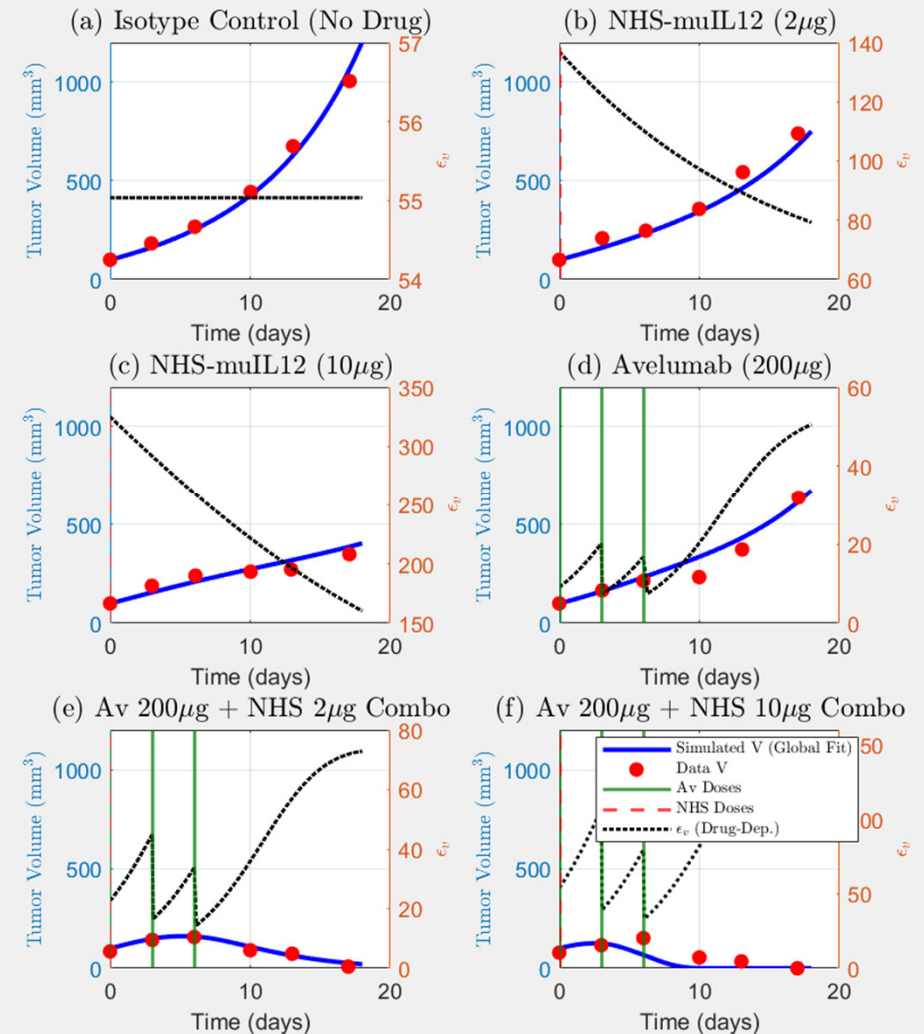


Epsilon as a function of treatment

$$\epsilon_v(t) = \epsilon \cdot \left(1 + \alpha_{NHS} \cdot \frac{A_{2n}}{K_{A2} + A_{2n}} \right) \cdot \left(\frac{1}{1 + \alpha_{Av} \cdot \frac{A_{1n}}{K_{A1} + A_{1n}}} \right)$$

- First term captures the tumor's **counter-adaptive response to immune stimulation** by NHS-muIL12. Tumor upregulates PD-L1 to try and evade immune system.
- Second term represents Avelumab's ability to **reduce the effective proportion of active PD-L1** on tumor cells.
- Epsilon set to 50 (Elpi's original value), so we only estimate the two alpha parameters.
- Note: another mechanism for the tumor's counter-adaptive response is *immune system exhaustion*.

4-ODE Model Global Fit (ϵ_v as Drug-Dependent Function)

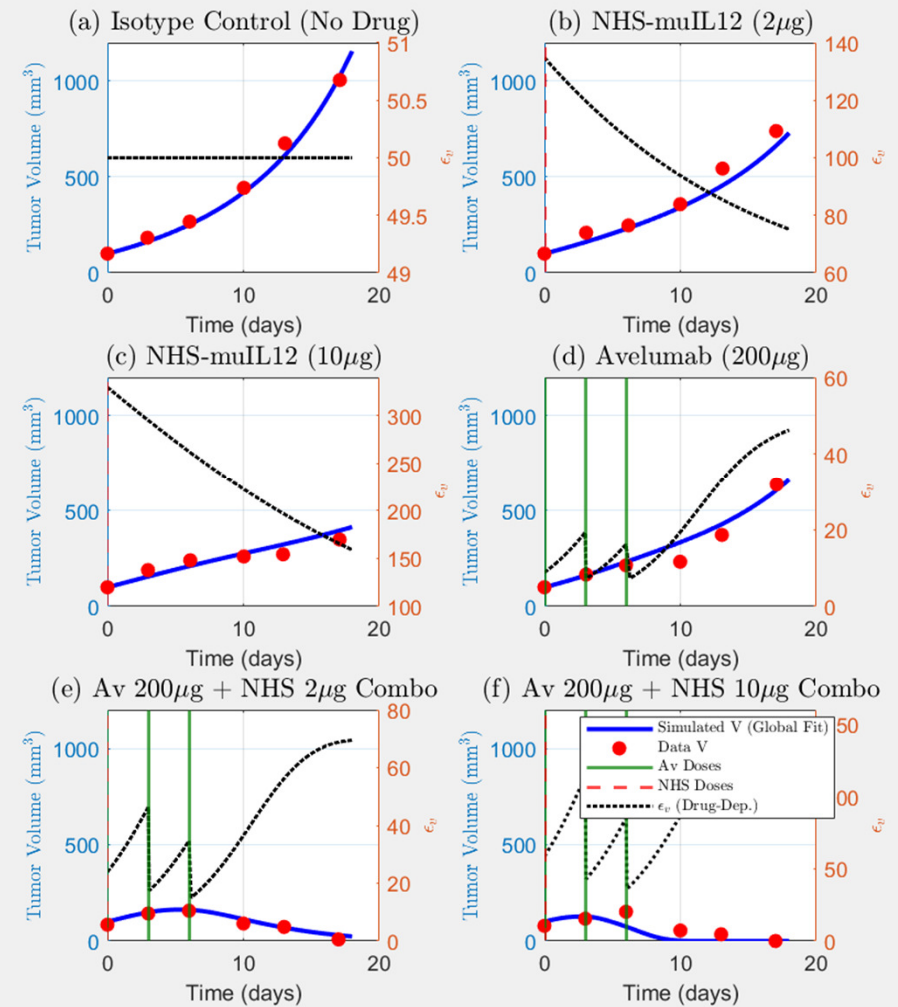


Excellent fittings

$$\epsilon_v(t) = \epsilon \cdot \left(1 + \alpha_{NHS} \cdot \frac{A_{2n}}{K_{A2} + A_{2n}} \right) \cdot \left(\frac{1}{1 + \alpha_{Av} \cdot \frac{A_{1n}}{K_{A1} + A_{1n}}} \right)$$

Estimate epsilon and the two alpha parameters.

4-ODE Model Global Fit (ϵ_v as Drug-Dependent Function)



Open Questions

- 1 Consider a more personalized approach by determining patient-specific parameters for each mouse.
- 2 Adapt the model to investigate the combination of different immune checkpoint inhibitors with other forms of treatment, such as chemotherapy.
- 3 Study the identifiability of the model.



Mathematical Modeling of an Immune Checkpoint Inhibitor and its Synergy with an Immunostimulant

Report

June 24, 2025



NAZARBAYEV
UNIVERSITY



Student Name:

Aigerim Kalizhanova

Data Extraction from Xu et al., 2017

To simulate and validate treatment strategies involving monotherapy and combination immunotherapy, I retrieved experimental data from Xu et al., 2017 using *WebPlotDigitizer*. Specifically, I extracted tumor volume data for the following treatment modes, which had outliers:

- **Mode 3:** Only NHS-muIL12 at $10\mu\text{g}$
- **Mode 5:** Avelumab + NHS-muIL12 at $2\mu\text{g}$
- **Mode 6:** Avelumab + NHS-muIL12 at $10\mu\text{g}$

The data consists of 2 mice groups with 8 individual mice in each, receiving different treatment strategies. The data was extracted for each individual, excluding the outliers. Further the data for each mode were averaged. The tumor volume dynamics for these three cases are shown below:

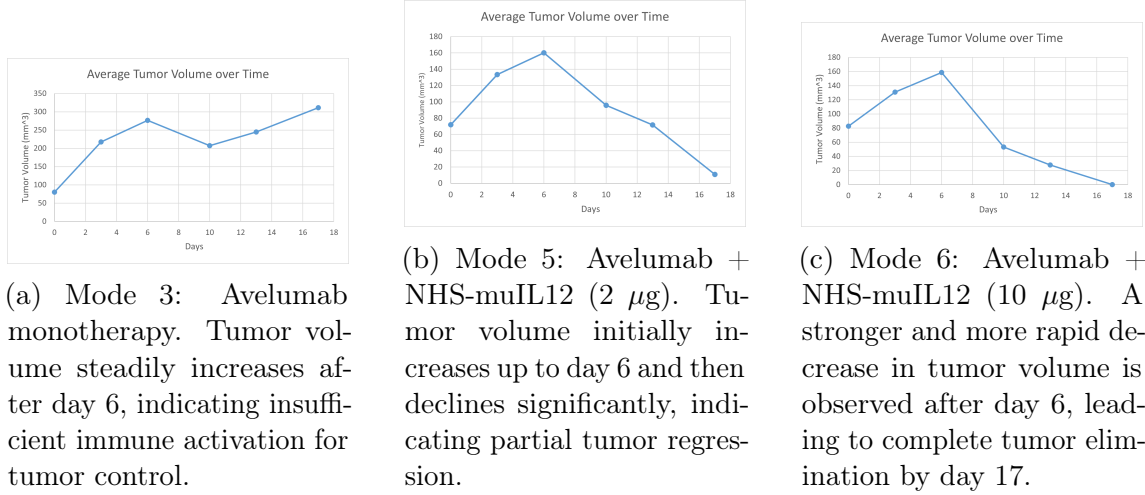


Figure 1: Tumor volume data extracted from Xu et al., 2017 for different treatment modes. Mode 3 shows monotherapy with avelumab, while Modes 5 and 6 represent combination therapies with increasing doses of NHS-muIL12.

Model Adjustments Based on CD8^+ T Cell Dynamics

The modification I propose is to change the activation rate of T cells by IL-12 and adjust the degradation rates. The reason is that the paper by Xu et al., 2017, where we retrieved the data using WebPlotDigitizer, focuses solely on CD8^+ T cells, which are responsible for directly killing tumor cells.

In the model presented by Nikolopoulou et al., 2021, which we are trying to improve, a single activation rate λ_{TI12} is used for all T cells (CD8^+ and CD4^+). The value for this rate, $\lambda_{\text{TI12}} = 8.81 \text{ day}^{-1}$, was adopted from Lai and Friedman, 2017, where the individual contributions were:

- $\lambda_{T8II2} = 4.15 \text{ day}^{-1}$ for $CD8^+$ T cells,
- $\lambda_{T1II2} = 4.66 \text{ day}^{-1}$ for $CD4^+$ T cells.

Since Xu et al.'s data is based on $CD8^+$ cells only, I propose to use only $\lambda_{T8II2} = 4.15 \text{ day}^{-1}$.

Degradation Rate Correction

In addition to this, I propose updating the degradation rates of Avelumab (A_1) and NHS-muIL12 (A_2). The original model by Nikolopoulou et al., 2021 used:

$$\begin{aligned} d_{A1} &= 0.1136 \text{ day}^{-1}, \quad (\text{half-life: } 6.1 \text{ days}) \\ d_{A2} &= 0.69 \text{ day}^{-1}, \quad (\text{half-life: } 1 \text{ day}) \end{aligned}$$

These values were derived from human data. However, the tumor data used for model validation comes from mouse experiments, making this parameter choice inconsistent.

Mouse-specific literature provides the following more accurate values:

- Avelumab: half-life $\approx 44.6 \text{ hours} = 1.86 \text{ days} \Rightarrow d_{A1} \approx 0.3726 \text{ day}^{-1}$ (Zalba et al., 2020);
- NHS-muIL12: half-life $\approx 9.5 \text{ days} \Rightarrow d_{A2} \approx 0.0730 \text{ day}^{-1}$ (Unverdorben et al., 2015).

By implementing these corrected values, we aim to achieve more physiologically accurate simulations of drug concentration and clearance, which in turn may improve the timing and magnitude of immune activation and tumor suppression in the model.

Results and Discussion

In this section, I introduce the results of these modifications. I would like to first note that the change in mentioned parameters had no effect on the parameters being fitted to the isotype control case: $\eta_1 = 8.83703e^{-01}$, $r = 2.00000e^{-01}$. However, there was a significant change in the behavior of the model for modes 3, 5 and 6 as presented in the Figure 2.

Our simulations in Figure 2b and 2d show qualitatively similar trends as those in the original Figure 2b and 2d in the work by Nikolopoulou et al., 2021. However, the updated model slightly underestimates tumor volume at later time points for mode 2 and overestimates it for mode 4. This could be attributed to the slower clearance of NHS-muIL12 in mice, which enhances its long-term immunostimulatory effect. For mode 3, both the original and updated models show minimal improvement in tumor suppression despite the increased dose ($10 \mu\text{g}$). However, our results display a slightly delayed tumor shrinkage onset. This might reflect that T cell activation saturates early, making dose escalation beyond $2 \mu\text{g}$ marginally effective in isolation.

Mode 5 (Figure 2e) shows modest tumor volume reduction after day 6, aligning better with the data extracted from Xu et al., 2017. This contrasts with Nikolopoulou's

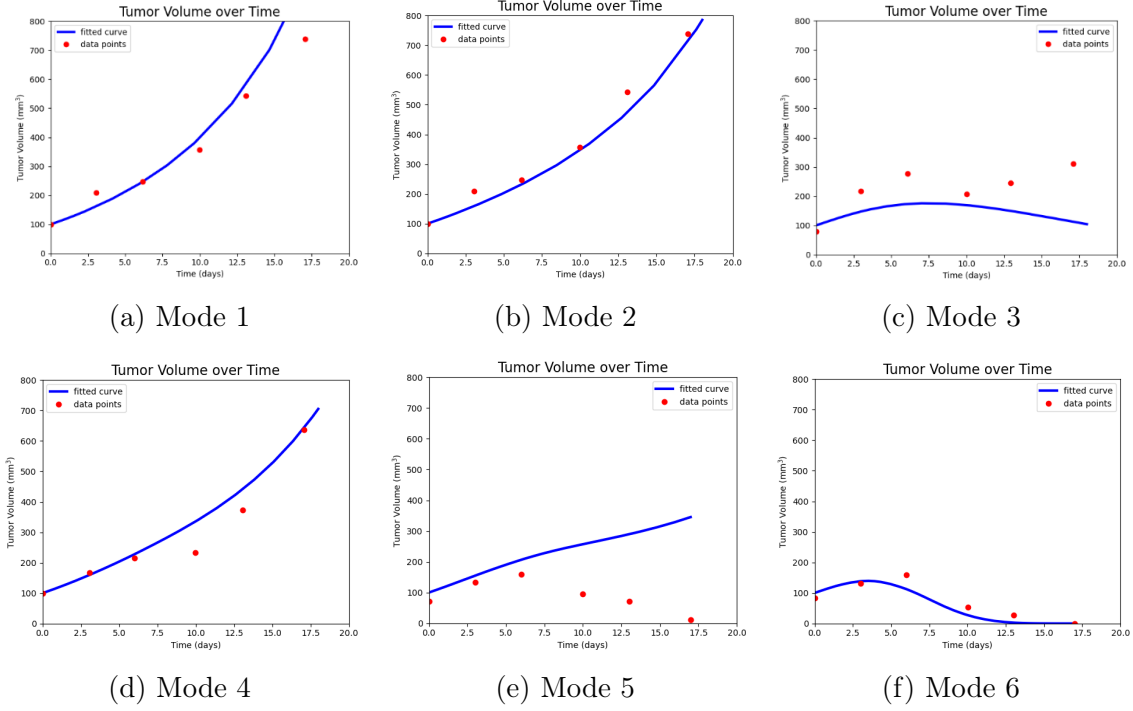


Figure 2: Tumor volume simulations using updated drug degradation rates: $d_{A_1} = 0.3726 \text{ day}^{-1}$, $d_{A_2} = 0.0730 \text{ day}^{-1}$ and the T cell activation activation rate $\lambda_{TI12} = 4.15$. The model was re-fitted with $\eta_1 = 8.83703 \times 10^{-1}$ and $r = 2.00000 \times 10^{-1}$.

original model (Figure 2e), where tumor suppression was underestimated. Mode 6 (Figure 2f) demonstrates effective tumor elimination by day 17, which closely mirrors the experimental data. The original model (Figures 2e, 3 left) fails to capture this full regression, likely due to underestimated IL-12 activation efficiency and overestimated degradation.

Overall, the monotherapy cases (modes 2 and 4) and the isotype control (mode 1) remain qualitatively consistent with previous model expectations. The tumor volume remains largely uncontrolled in these modes, as expected from limited or no therapeutic intervention. The updated model improves both biological relevance and predictive performance, particularly for the most clinically relevant combination therapies. These adjustments address prior limitations in parameter assumptions and better reflect the experimental conditions under which the data were obtained.

References

- Lai, X., & Friedman, A. (2017). Combination therapy of cancer with cancer vaccine and immune checkpoint inhibitors: A mathematical model. *PLoS ONE*, *12*(5), e0178479. <https://doi.org/10.1371/journal.pone.0178479>
- Nikolopoulou, E., Eikenberry, S. E., Gevertz, J. L., & Kuang, Y. (2021). Mathematical modeling of an immune checkpoint inhibitor and its synergy with an immunostimulant. *Discrete and Continuous Dynamical Systems - Series B*, *26*(4), 2133–2159. <https://doi.org/10.3934/dcdsb.2020138>
- Unverdorben, F., Richter, F., Hutt, M., Seifert, O., Malinge, P., Fischer, N., & Kontermann, R. E. (2015). Pharmacokinetic properties of IgG and various Fc fusion proteins in mice. *mAbs*, *8*(1), 120–128. <https://doi.org/10.1080/19420862.2015.1113360>
- Xu, C., Zhang, Y., Rolfe, P. A., Hernández, V. M., Guzman, W., Kradjian, G., Marelli, B., Qin, G., Qi, J., Wang, H., Yu, H., Tighe, R., Lo, K.-M., English, J. M., Radvanyi, L., & Lan, Y. (2017). Combination Therapy with NHS-muIL12 and Avelumab (anti-PD-L1) Enhances Antitumor Efficacy in Preclinical Cancer Models. *Clinical Cancer Research*, *23*(19), 5869–5880. <https://doi.org/10.1158/1078-0432.ccr-17-0483>
- Zalba, S., Contreras-Sandoval, A. M., Martisova, E., Debets, R., Smerdou, C., & Garrido, M. J. (2020). Quantification of pharmacokinetic profiles of PD-1/PD-L1 antibodies by validated ELISAs. *Pharmaceutics*, *12*(6), 595. <https://doi.org/10.3390/pharmaceutics12060595>

To Optimize Treatment, we Need Reliable Models.

- Different parameter values may describe the data equally well.
- Predictions are highly sensitive to unmeasurable variables, especially those affecting the model dynamics.

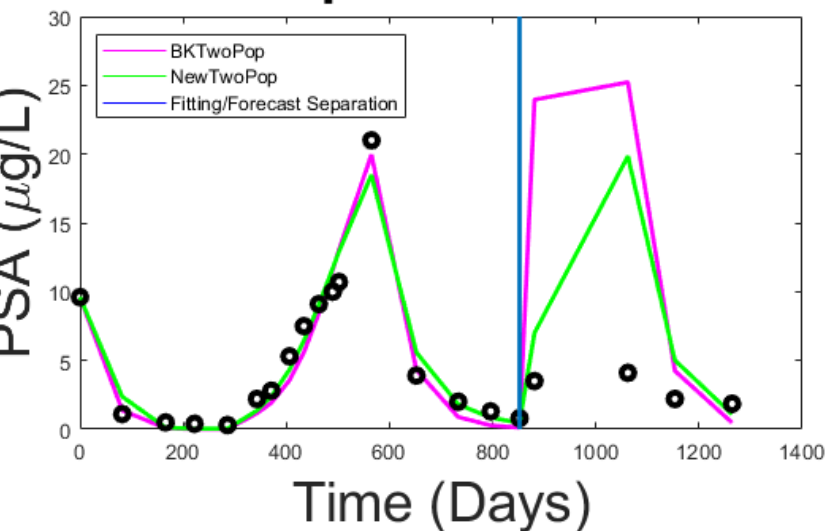
\implies Identifiability is important!

Acknowledgment

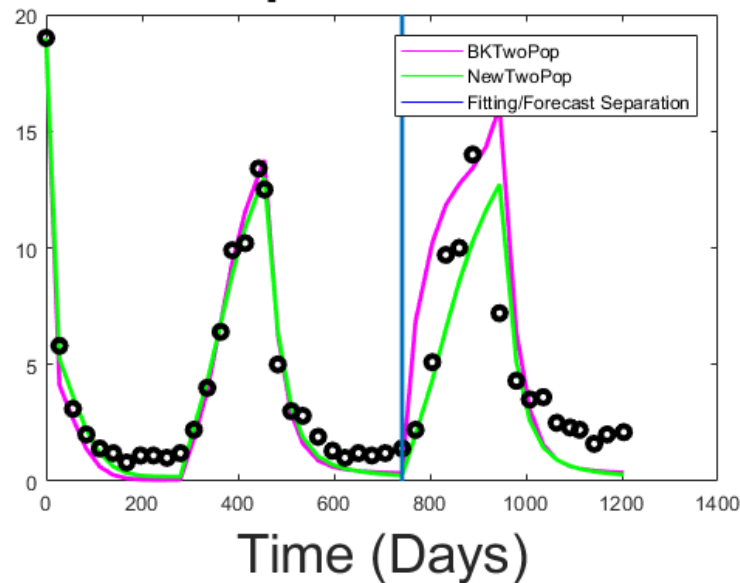
Research of YK is partially supported by NSF grants DMS-1615879, DEB-1930728 and an NIH grant 5R01GM131405-02.

THANK YOU!

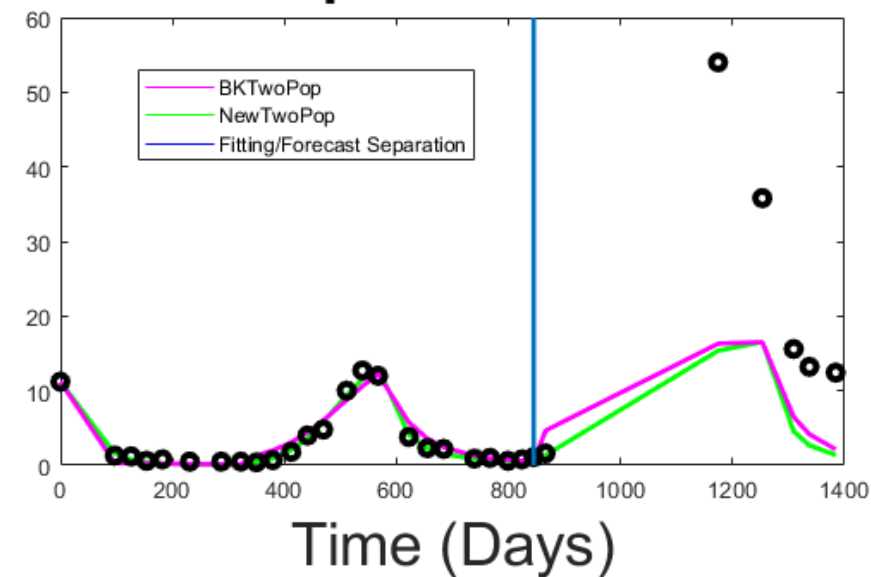
patient36



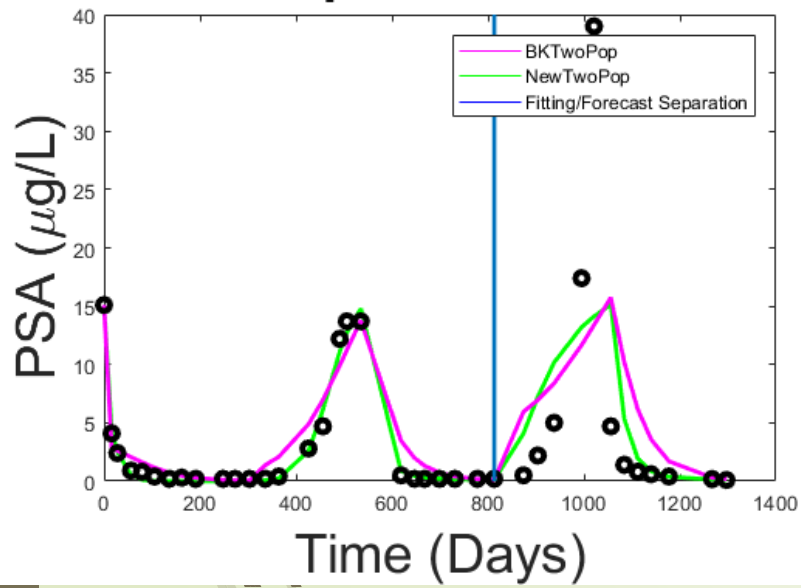
patient39



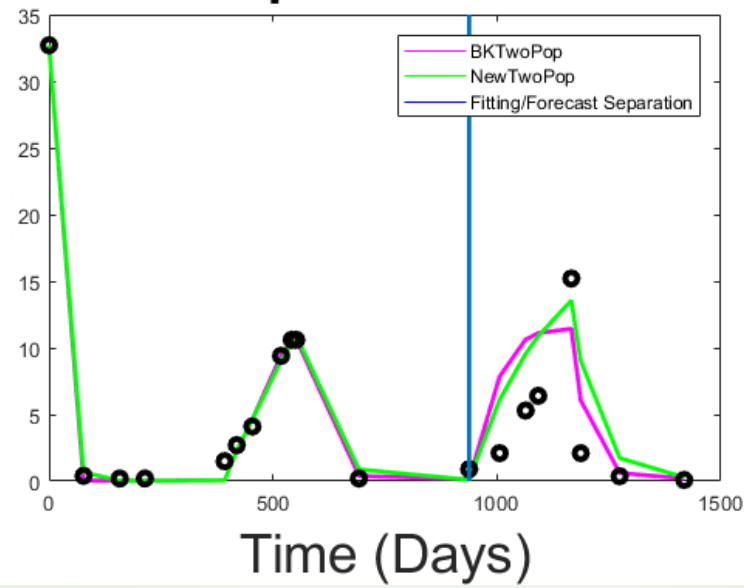
patient54



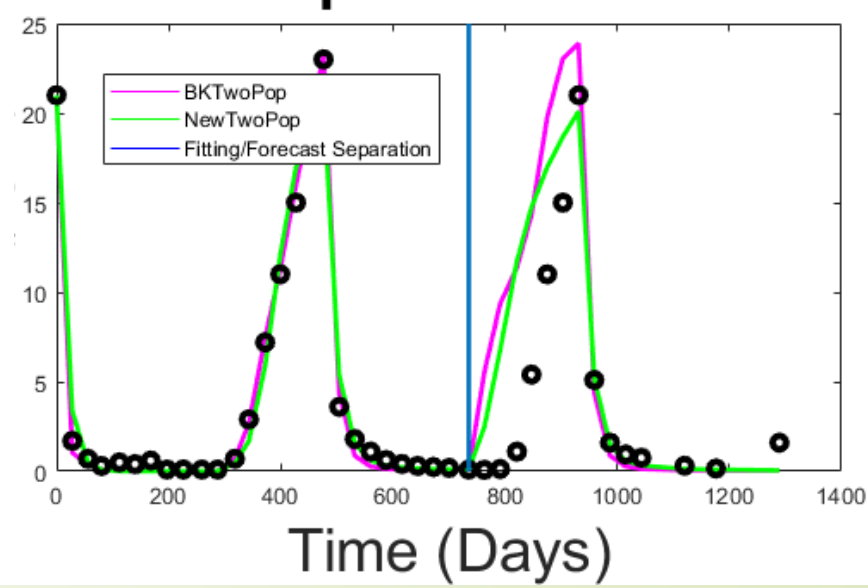
patient60



patient62



patient77



New Two Population Model

$$\Rightarrow x_1' = \mu_m \left(1 - \frac{q_1}{Q}\right) x_1 - (D_1(Q) + \delta_1 x_1) x_1 - \lambda(Q) x_1$$

$$\Rightarrow x_2' = \mu_m \left(1 - \frac{q_2}{Q}\right) x_2 - (D_2(Q) + \delta_2 x_2) x_2 + \lambda(Q) x_1$$

$$\Rightarrow Q' = \gamma(A - Q) - \frac{\mu_m(Q - q_1)x_1 + \mu_m(Q - q_2)x_2}{x_1 + x_2}$$

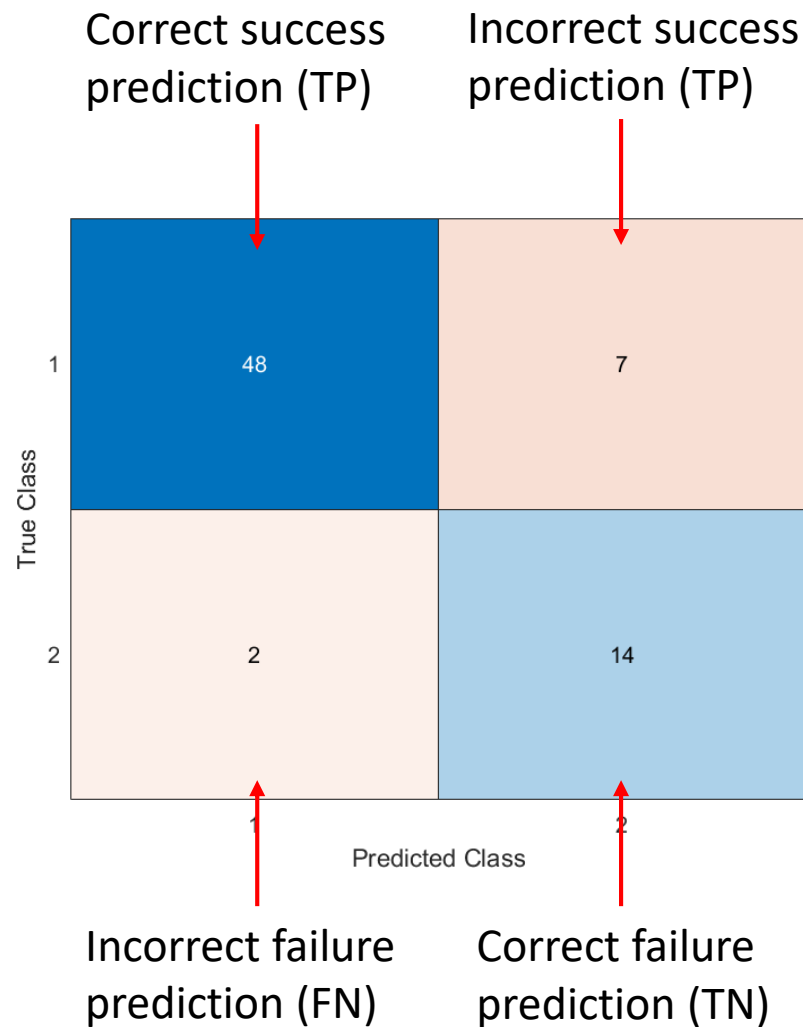
$$\Rightarrow A' = c_1(A_0 - A) - c_1 A_0(1 - u)$$

$$\Rightarrow P' = bQ + \sigma(Qx_1 + Qx_2) - \varepsilon P$$

$$\Rightarrow D_i(Q) = d \frac{R_i}{Q + R_i}, \quad \lambda(Q) = c \frac{K}{Q + K}$$

$$\Rightarrow \gamma = \gamma_1 u(t) + \gamma_2$$

$$\Rightarrow u(t) = \begin{cases} 0, & \text{on treatment} \\ 1, & \text{off treatment} \end{cases}$$



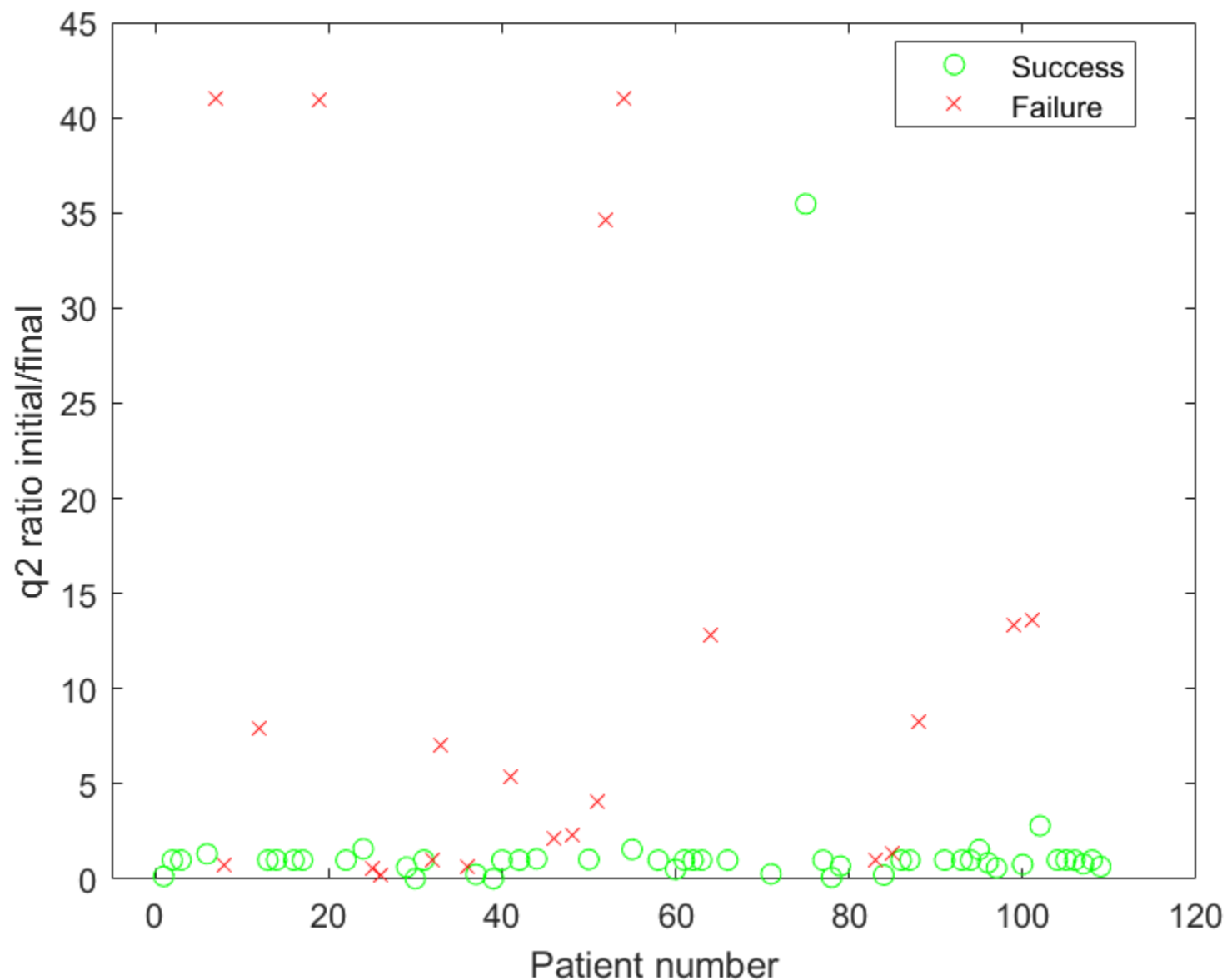
With a threshold of 2.0

Sensitivity = $48/55 = 87.3\%$

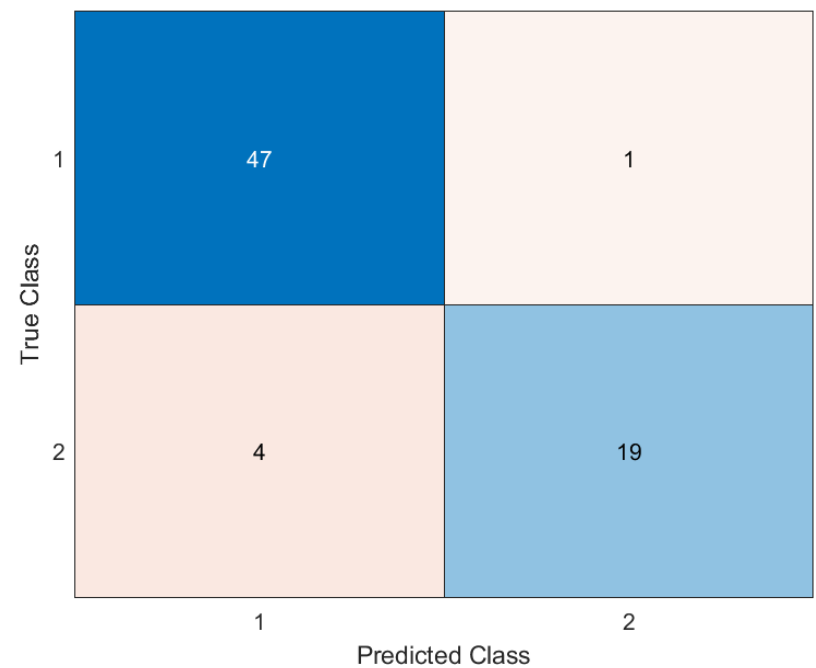
Specificity = $14/16 = 87.5\%$

Accuracy = $62/71 = 87.3\%$

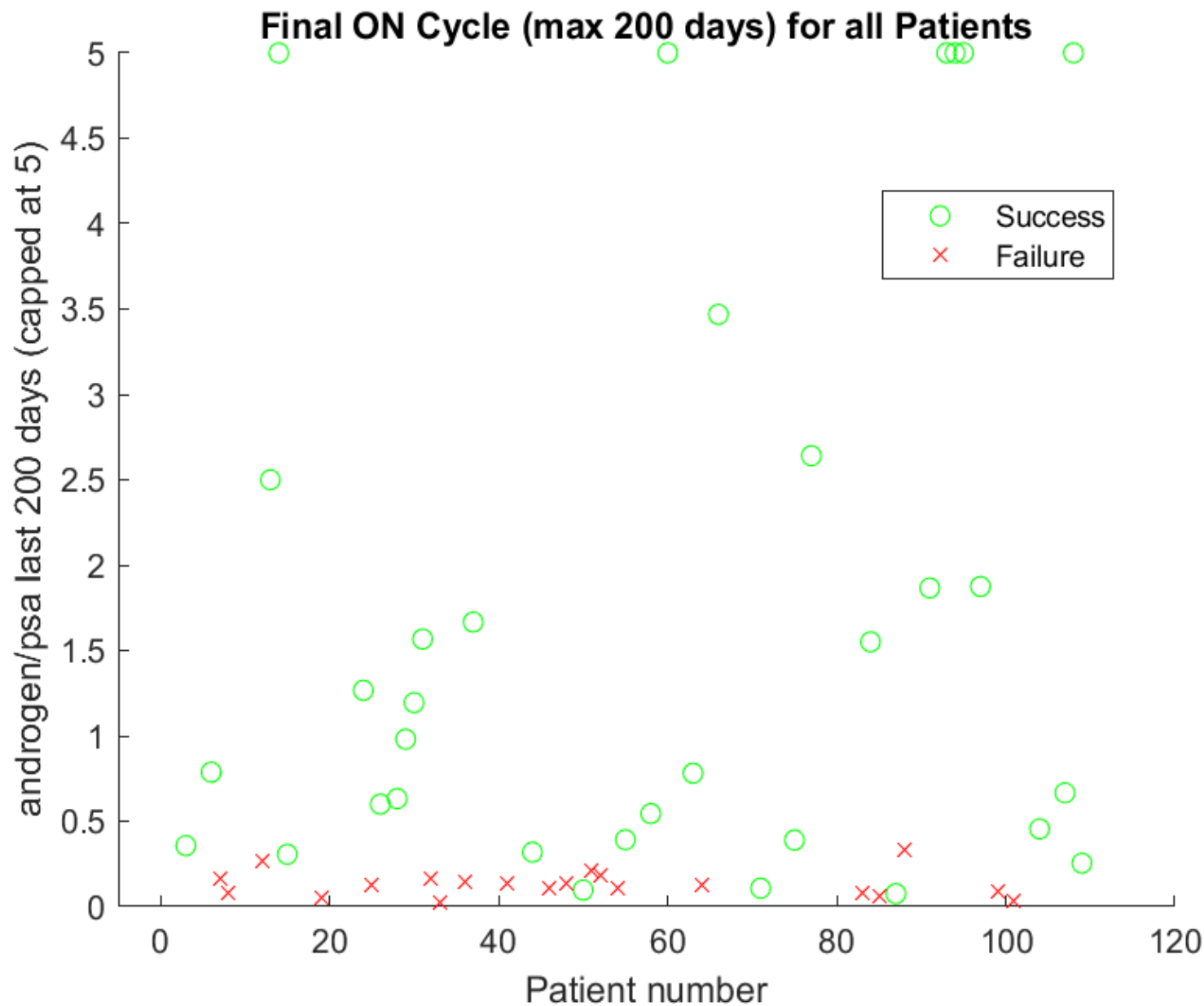
Predicting Treatment Outcome



Predicting Treatment Outcome



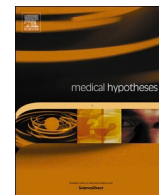
With a threshold of .27
Sensitivity = 47/48 = 97.9%
Specificity = 19/23 = 82.6%
Accuracy = 62/71 = 93.0%





Contents lists available at ScienceDirect

Medical Hypotheses

journal homepage: www.elsevier.com/locate/mehy

The prognostic value of androgen to PSA ratio in predictive modeling of prostate cancer

Tin Phan^{a,*}, Allison Weber^b, Alan H. Bryce^c, Yang Kuang^d

^a Theoretical Biology and Biophysics T-6, Los Alamos National Laboratory, Los Alamos, NM 87545, USA

^b College of Computing, Georgia Institute of Technology, Atlanta, GA 30332, USA

^c Division of Hematology and Medical Oncology, Mayo Clinic Cancer Center, Phoenix, AZ 85054, USA

^d School of Mathematics and Statistical Sciences, Arizona State University, Tempe, AZ 85281, USA

ARTICLE INFO

Keywords:

Prostate cancer

Predictive modeling

Hormonal treatment

Androgen deprivation therapy

PSA

Androgen

ABSTRACT

Prostate specific antigen (PSA) is the ubiquitous biomarker used in mathematical and artificial intelligence models of prostate cancer. Yet, it is imperfect. The growth of prostate and cancer cells produces PSA, but their growth is dependent on androgen in most cases. Thus, looking at PSA by itself ignores the impact of androgen. Here, we propose the use of androgen as a reference framework for better integration of PSA in prostate cancer models. The binding of androgen to androgen receptors activates signals that promote prostate cancer growth and the production of PSA, so higher levels of androgen should correlate to higher growth of the tumor and higher production of PSA. Thus, PSA and androgen fall and rise almost synchronously during the start and stop of androgen deprivation therapy (ADT), respectively. Yet, when cancer cells become resistant to ADT, we observe a divergence to this trend, leading to a high level of PSA even during ADT. Therefore, we hypothesize that the cancer evolutionary dynamics can be represented by the ratio of androgen to PSA and its integration into prostate cancer models may help improve their predictive power.

Subject: PSA/androgen update

From: "Phan, Tin Thien" <ttphan@lanl.gov>

Date: 6/25/2025, 3:46 PM

To: Yang Kuang <kuang@asu.edu>, John Nagy <john.nagy@asu.edu>, "wmeade@asu.edu" <wmeade@asu.edu>

Hi all,

In case you have not seen this, the Moffitt Cancer Center put out this preprint last month.

<https://www.medrxiv.org/content/10.1101/2025.05.08.25327179v1>

There is another clinical study that I'm reviewing for supporting our finding of using PSA/androgen.

Best,

Tin

Model 1: AD Population



$$\frac{dX_1}{dt} = \alpha_1 p(A) X_1 - \beta_1 q(A) X_1 - m(A) X_1$$

$$p(A) = \frac{A}{A + k_1}$$

Proliferation

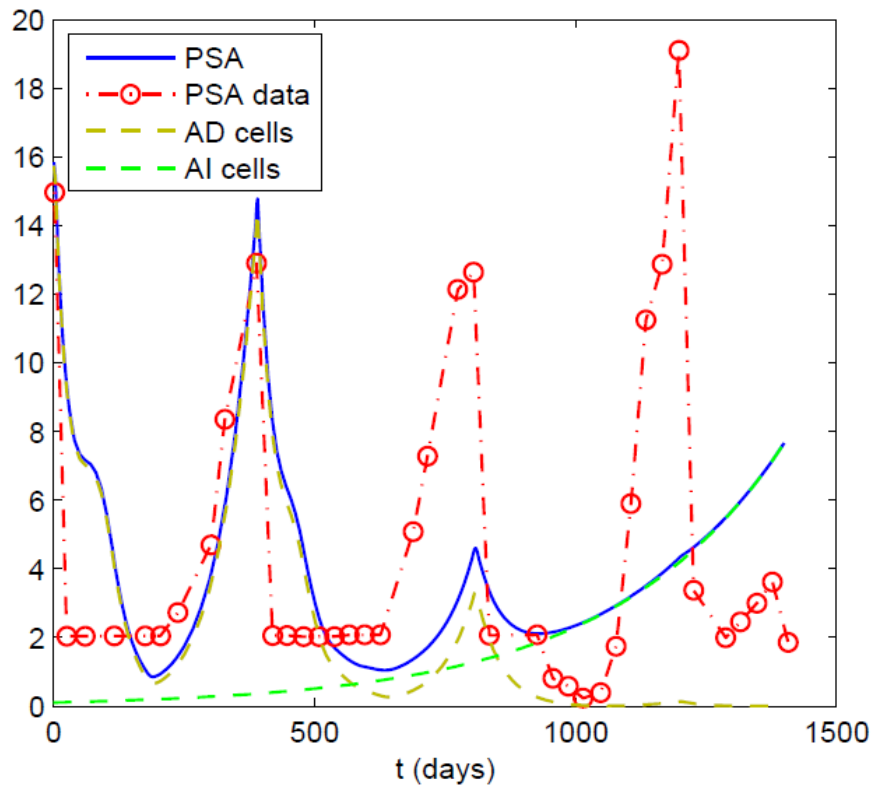
$$q(A) = k_2 + (1 - k_2) \frac{A}{A + k_3}$$

Death, $k_2 > 1$

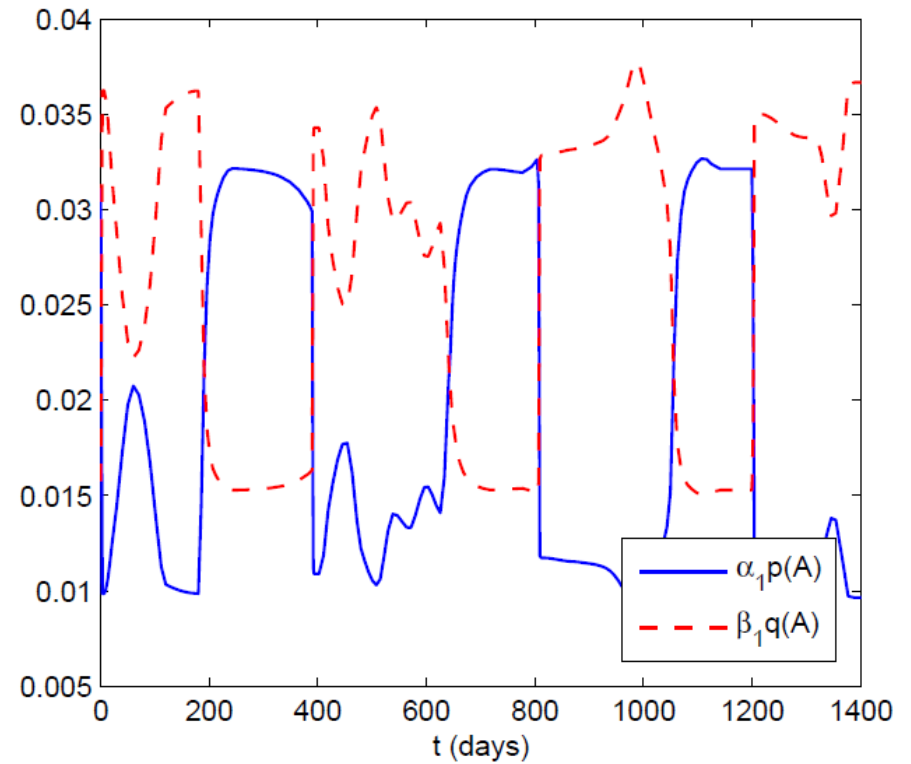
$$m(A) = m_1 \left(1 - \frac{A}{a_0} \right)$$

Mutation

Model 1



Case 1



Growth and death rates



Home | Curriculum Vitae | Curriculum Vitae Abbreviated | Biography | Lab Notes | Clinical Research



Nicholas Bruchofsky, MD, PhD, FRCPC

NICHOLAS BRUCHOVSKY, MD, PhD, FRCPC September 21, 1936 - March 22, 2015

Clinical data can be downloaded at:
<http://www.nicholasbruchovsky.com/clinicalResearch.html>

Home | Curriculum Vitae | Curriculum Vitae Abbreviated | Biography | Lab Notes | Clinical Research

© Copyright 2005. Nicholas Bruchofsky.

Introduction to Mathematical Oncology

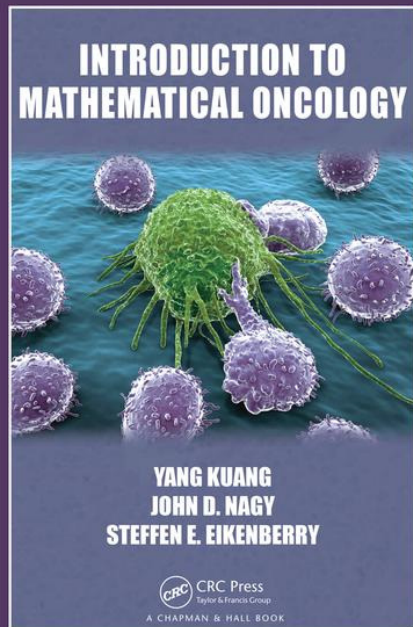
Yang Kuang, John D. Nagy, Steffen E. Eikenberry

February 18, 2016 by Chapman and Hall/CRC

Textbook - 470 Pages - 77 B/W Illustrations

ISBN 9781584889908 - CAT# C990X

Series: [Chapman & Hall/CRC Mathematical and Computational Biology](#)



For Instructors

[Request an e-inspection copy](#)

Select Format:

Hardback

Quantity: